REMARKS

Status of the Claims

Claims 1-20 are pending in this application. Claims 15-20 have been withdrawn from consideration. No claims have been canceled, added or amended.

Rejection under 35 USC 112, first paragraph

The Examiner rejects claims 1-14 as not enabled by the specification. The Examiner states that all compounds that bind to the SS1 and SS2 subunits of a sodium channel are not enabled by the specification. The Examiner states that only tetrodotoxin, saxitoxin and derivatives thereof are enabled. Applicants traverse the rejection and respectfully request the withdrawal thereof.

Applicants submit that the Examiner has failed to meet the burden of presenting a *prima facie* case as to why the claims would not be enabled. See *In re Wright*, 27 USPQ2d 1510 (Fed. Cir. 1993). *Wright*, citing *In re Marzocchi*, 169 USPQ 367, 369 *(CCPA 1971)* states

> *When rejecting a claim under the enablement requirement of section 112, the PTO bears an initial burden of setting forth a reasonable explanation as to why it believes that the scope of protection provided by that claim is not adequately enabled by the description of the invention provided in the specification of the application; this includes, of course, providing sufficient reasons for doubting any assertions in the specification as to the scope of enablement. If the PTO meets this burden, the burden then shifts to the applicant to provide suitable proofs indicating that the specification is indeed enabling.*

The Examiner has failed to meet this initial burden.

Even if the Examiner had met this burden, Applicants have submit that the present specification provides adequate enablement. It is not necessary that the specification provide examples of every possible operable embodiment, only that the specification, taken with what was known at the time the application was filed, describe to the skilled artisan how embodiments throughout the scope of the claims can be made without undue experimentation.

The present specification describes a number of compounds effective in the present invention, and this is acknowledged by the Examiner. Furthermore, Applicants also submit herewith evidence that establishes that the state of the art at the time the application was filed was such that certain structural and functional similarities between compounds that bind SS1 and SS2 subunits were recognized. Applicants submit that one of ordinary skill in the art would be able to identify compounds that bind SS1 and SS2 subunits for use in the present invention. Absent a preponderance of evidence from the Examiner that the skilled artisan could not identify compounds that bind to SS1 and SS2 subunits that work in the present invention, a

presumption arises that the full scope of the claimed invention is enabled by the specification.

Applicants submit herewith three journal articles: Yang, L. et al. "Actions of Chiriquitoxin on Frog Skeletal Muscle Fibers and Implications for the Tetrodotoxin/Saxitoxin Receptor", Journal of General Physiology, Vol. 100, pages 609 to 622, published October 1992; Fozzard, H. et al., "The Guanidinium Toxin Binding Site on the Sodium Channel", Japanese Heart Journal, Vol. 37, No. 5, pages 683 to 692, published September 1996; and Lipkind, G. et al., "A Structural Model of the Tetrodotoxin and Saxitoxin Binding Site of the Na+ Channel", Biophysical Journal, Vol. 66., pages 1 to 13, published January 1994. Each of these references supports Applicants' position that the claims are enabled.

For example Lipkind et al. describes a three dimensional model of the SS1 and SS2 subunits with TTX bound thereto. The model is so detailed as to show contacts of the toxin with the protein. Such a detailed model allows the skilled artisan to predict the structure of an effective sodium channel blocker. The authors state in the introduction that TTX and STX have virtually identical biological activity due to a common guanidinium group that is positively charged at physiological pH. The authors note that a guanidinium group is common to compounds that bind SS1 and SS2

subunits of the sodium channel and is important for blocking the channel.

See also the Abstract of Yang et al., which discloses that chiquirotoxin (CqTX), another sodium channel blocker, is only different from TTX in the substitution of a glycine residue in place of a methylene hydrogen of the C-11 hydroxyl methyl function.

Lastly, Fozzard et al. explains that guanidinium is a common feature of compounds that bind to the sodium channel.

Applicants submit that compounds that bind to SS1 and SS2 subunits of the sodium channel are easily determined without undue experimentation, particularly given knowledge of a chemical structure that is a feature of such compounds. A guanidinium group is likely to be present in an effective compound. This knowledge provides a starting point for any expected experimentation. To this knowledge, Yang et al. add a technique for determining effectiveness of the compounds selected. Yang et al. use the patch clamp method to measure the channel current in the presence and absence of an inhibitor.

The state of the art at the time the application was filed was thus such that the skilled artisan could predict the structure of a SS1 or SS2 -binding sodium channel blocker and could test that compound for effectiveness using assays known in the art. Thus, no undue experimentation is required to practice the present invention

throughout the scope of the present claims. Therefore, Applicants submit that the claims are enabled and the instant rejection should be withdrawn.

Conclusion

As Applicants have addressed and overcome the rejection in the Office Action, Applicants respectfully request that the rejection be withdrawn and that the claims be allowed.

Should there be any outstanding matters that need to be resolved in the present application, the Examiner is respectfully requested to contact Kecia Reynolds (Reg. No. 47,021) at the telephone number of the undersigned below, to conduct an interview in an effort to expedite prosecution in connection with the present application.

If necessary, the Commissioner is hereby authorized in this, concurrent, and future replies, to charge payment or credit any overpayment to Deposit Account No. 02-2448 for any additional fees required under 37 C.F.R. §§ 1.16 or 1.17; particularly, extension of time fees.

Respectfully submitted,

BIRCH, STEWART, KOLASCH & BIRCH, LLP

By _____
Mark J. Nuell, #36,623

P.O. Box 747
Falls Church, VA 22040-0747
(703) 205-8000

DRN/KJR/jao

Attachment(s): Lipkind et al.
Yang et al.
Fozzard et al.

(Rev. 09/30/03)

Biophysical Journal Volume 66 January 1994 1–13

A Structural Model of the Tetrodotoxin and Saxitoxin Binding Site of the Na^+ Channel

2003.11.13

Gregory M. Lipkind and Harry A. Fozzard

The Cardiac Electrophysiology Laboratories, and The Departments of Pharmacological and Physiological Sciences, Biochemistry and Molecular Biology and Medicine, The University of Chicago, Chicago, Illinois 60637 USA

ABSTRACT Biophysical evidence has placed the binding site for the naturally occurring marine toxins tetrodotoxin (TTX) and saxitoxin (STX) in the external mouth of the Na^+ channel ion permeation pathway. We developed a molecular model of the binding pocket for TTX and STX, composed of antiparallel β-hairpins formed from peptide segments of the four S5–S6 loops of the voltage-gated Na^+ channel. For TTX the guanidinium moiety formed salt bridges with three carboxyls, while two toxin hydroxyls (C9-OH and C10-OH) interacted with a fourth carboxyl on repeats I and II. This alignment also resulted in a hydrophobic interaction with an aromatic ring of phenylalanine or tyrosine residues for the brainII and skeletal Na^+ channel isoforms, but not with the cysteine found in the cardiac isoform. In comparison to TTX, there was an additional interaction site for STX through its second guanidinium group with a carboxyl on repeat IV. This model satisfactorily reproduced the effects of mutations in the S5–S6 regions and the differences in affinity by various toxin analogs. However, this model differed in important ways from previously published models for the outer vestibule and the selectivity region of the Na^+ channel pore. Removal of the toxins from the pocket formed by the four β-hairpins revealed a structure resembling a funnel that terminated in a narrowed region suitable as a candidate for the selectivity filter of the channel. This region contained two carboxyls (Asp^{384} and Glu^{942}) that substituted for molecules of water from the hydrated Na^+ ion. Simulation of mutations in this region that have produced Ca^{2+} permeation of the Na^+ channel created a site with three carboxyls (Asp^{384}, Glu^{942}, and Glu^{1714}) in proximity.

INTRODUCTION

Tetrodotoxin (TTX) and saxitoxin (STX) are naturally occurring high affinity marine toxins that selectively block the voltage-sensitive Na^+ channel (Hille, 1992; Catterall, 1992). Their overlapping binding sites are most probably located in the outside mouth of the ion permeation pathway. Although the chemical structures of TTX and STX (see Fig. 1) are quite different, their biological activities are virtually identical, partly as a consequence of a shared guanidinium group that is positively charged at physiological pH. One or more negatively charged carboxyl groups on the channel protein have been shown to play an essential role in toxin binding by either pH titration or by treatment with carboxyl-modifying reagents (Hille, 1968; Shrager and Profera, 1973). The guanidinium ion itself is permeant to the Na^+ channel (Hille, 1971), and both permeant and non-permeant (blocking) cations can compete for the toxin site (Narahashi, 1974). On the basis of such data, Hille (1975) suggested that the guanidinium group of TTX is bound to a rectangular ring of six oxygens located in the walls of the channel pore at its selectivity filter, with the cationic guanidinium forming a salt bridge to one negatively charged acid group and with other polar groups of the toxin interacting with the remaining oxygens so as to occlude the pore.

In 1984 Numa and coworkers (Noda et al., 1984) cloned the first of a family of isoforms of the principal subunit of the Na^+ channel. These Na^+ channel α-subunits are large glycoproteins of about 2000 amino acids, organized into four highly homologous domains or repeats (I–IV). Each domain includes six transmembrane segments (S1–S6) with high α-helical potential (Numa and Noda, 1986). On the basis of biophysical and chemical data the extracellular segment between S5 and S6 of each repeat is thought to fold back into the membrane to form part of the ion-conducting pathway (Guy and Conti, 1990). A series of point mutations in this S5–S6 segment by Stühmer, Numa, and colleagues and others (Noda et al., 1989; Terlau et al., 1991; Satin et al., 1992; Backx et al., 1992; Heinemann et al., 1992a; Kontis and Goldin, 1993) has identified several specific amino acids essential for toxin block and for isoform differences in toxin affinity.

The size and solubility characteristics of the Na^+ channel preclude determination of the three-dimensional structure of this large molecule at this time. However, the primary structures of several isoforms are known, along with effects of point mutations that affect toxin binding. We used this information to develop a model of the toxin binding pocket from parts of the S5–S6 loops that have been identified as probable parts of the outer vestibule of the channel pore. The model was based on the simple question if a reasonable structural organization of the amino acids in this region could be arranged around the toxin molecules so as to form an interaction that satisfied the available analog and mutation data. Working with only a small fraction of the entire protein sequence, we found a predicted structure of these short peptide

Received for publication 22 July 1993 and in final form 12 October 1993.
Address reprint requests to Dr. Harry A. Fozzard at MC 6094, 5841 S. Maryland Ave., Chicago, IL 60637. Tel.: 312-702-1481; fax: 313-702-6789.

0006-3495/94/01/01/13 $2.00

segments that interacted well with the toxins, yielding a binding pocket conforming to the available experimental toxin analog and channel point mutation data and to channel isoform differences in toxin block.

EXPERIMENTAL RESULTS USED IN MODEL DEVELOPMENT

The construction and constraints of this model depend strongly on experimental studies of block by toxins and their analogs, and on the available data on point mutations in cloned Na^+ channels.

Blockade by various guanidinium toxins

Kao and coworkers (see review by Kao, 1986) have identified the active groups in TTX and STX. In the case of TTX these are the guanidinium group and the hydroxyls at C9 and C10 (see Fig. 1). The guanidinium group is thought to form an ion-pair with an anionic site of the receptor, while the C9-OH and C10-OH form hydrogen bonds with other sites (Kao and Walker, 1982). The latter suggestion was confirmed by the low (0.01–0.02 ×) affinity of the analog anhydrotetrodotoxin, where C4 and C9 are joined by an oxygen bridge (Narahashi et al., 1967; Kao and Yasumoto, 1985). 4-Epitetrodotoxin, in which the positions of the -H and -OH were reversed from TTX, is about 0.5 × as potent as TTX. Therefore, the change in activity of anhydrotetrodotoxin can be explained as loss of the C9-OH group and one of the hydrogen bonds to the binding site. Modifications of both C9-OH and C10-OH in the case of tetrodonic acid led to a totally ineffective molecule (Narahashi et al., 1967). 6-Epitetrodotoxin and 11-deoxytetrodotoxin have low binding affinity (about 0.01 ×) to Na^+ channels (Yang et al., 1992a). However, nortetrodotoxin and nortetrodotoxin alcohol, which cannot form corresponding hydrogen bonds, were somewhat less potent than TTX (Kao, 1982), implying that the C6 end of TTX is not very important for channel block.

In prior studies of STX, the 7,8,9-guanidinium group and two C12 hydroxyls were identified as important for STX binding (Strichartz, 1984; Kao, 1986). The two hydroxyls can be reduced selectively to produce either the α or the β epimer of saxitoxinol, which have blocking affinity of only 0.01 × (Koehn et al., 1981; Kao et al., 1985). Koehn et al. (1981) concluded that the carbamoyl group of STX (H_2NCO-group as substitute at C6) contributes to, but is not essential for channel blockade, because decarbamoylsaxitoxin (dcSTX) is about 0.2 × as active as STX. Besides, an acetyl derivative of dcSTX, in which an amino group was substituted by a methyl group, has shown the same activity (Mahar et al., 1991). Nevertheless, the potency of decarbamoyloxysaxitoxin is only 0.008 × that of STX (Yang et al., 1992b).

Yang and Kao (1992) identify seven possible interaction sites in the structures of TTX and STX that they conclude are important, but a more conservative analysis suggests that only the guanidinium group and the two hydroxyls at C9 and C10 (for TTX) or C12 (for STX) are the most critical sites. These sites show remarkable stereospecific similarities and appear to determine the high toxin specificity. When the guanidinium group of TTX and the 7,8,9-guanidinium group of STX are aligned, then the hydroxyls at C9 and C10 for TTX and the two hydroxyls at C12 for STX are also closely aligned (Kao and Walker, 1982). The positive charge in the second 1,2,3-guanidinium group of STX may also be involved, but direct evidence is lacking. Finally, chiriquitoxin (CqTX) differs from TTX only by a glycine residue in place of a hydrogen of the hydroxymethyl group at position C11, but at pH 7.25 it has equal block potency as TTX (Yang and Kao, 1992). Since glycine has high potency for formation of hydrogen bonds but its presence does not modify binding, the C11 site is most probably outside of the vestibule and not able to interact with the binding pocket.

Inference for binding from mutation studies

Site-directed mutations of the conserved amino acids of the rat brain II (rBrII), the adult skeletal, and the cardiac α-subunits of the Na^+ channel have provided important information about the amino acids residues required for TTX and STX binding. We are indebted to the extensive work of Stühmer, Numa, and colleagues for explorations of the amino acids previously suggested by Guy and Conti (1990) to be part of the pore and named SS1-SS2 or the P loop. A single point mutation of glutamic acid 387 (rBrII number) to glutamine (E387Q) results in complete loss of TTX and STX block (Noda et al., 1989). Glu^{387} belongs to the SS2 segment of repeat I (Fig. 2). Terlau et al. (1991) made systematic mutations in residues of the SS2 segments of repeats I–IV. Neutralization of any of the six conserved residues of Glu or Asp reduced the sensitivity to TTX and STX block by at least three orders of magnitude (Table 1). Charge mutations at other adjacent positions produced smaller changes in toxin block. Terlau et al. (1991) suggested that there are two clusters of negatively charged residues at equivalent positions in the SS2 segments of repeats I–IV (marked by *arrows* in Fig. 2). The most dramatic effect on toxin block in their study was produced by neutralization of the carboxyl residues on repeats I and II. Neutralization of aspartic acid at position 1717 of repeat IV (D1717N) abolished STX block, while partially

TABLE 1 Effects of single mutations on TTX and STX sensitivities and single channel conductance

Mutant	Repeat	IC_{50}, TTX	IC_{50}, STX	Conductance
		nM	nM	pS
Wild-type		18 ± 4	1.2 ± 0.2	15.4
D384N	I	>10000	>1000	<0.1
E387Q		>10000	>1000	3.1
E942Q	II	>10000	>1000	<0.5
E945Q		2800 ± 180	>1000	8.2
D1426N	III	30 ± 10	8.9 ± 0.4	14.0
D1717N	IV	350 ± 90	>1000	8.8

Data from Terlau et al. (1991).

reducing the block by TTX. In repeat III neutralization of Asp^{1426} (mutant D1426N) had little effect on either toxin. Finally, the cardiac isoform has a lower affinity for both toxins, which appears to be a consequence of the absence of an aromatic ring residue (Tyr or Phe) at position 385 in the rBrII number system (Satin et al., 1992; Backx et al., 1992; Heinemann et al., 1992a).

STRUCTURAL MOTIF FOR THE TTX/STX BINDING SITE

For this model we infer that a residue is involved in a non-bonding or electrostatic interaction with the toxin if its substitution changes the toxin blocking affinity 100–1000 ×. Effects on binding affinity less that 10 × can be physiologically interesting, but beyond the accuracy of the present model.

Scheme of principal sites of interaction

In agreement with the experimental results of Terlau et al. (1991), we assumed that similar structural elements of the two toxins interact with residues of repeats I and II (Table 1). The guanidinium group and the hydroxyls C9-OH and C10-OH of TTX and the 7,8,9-guanidinium group and the hydroxyls at C12 of STX interact primarily with carboxyls at positions 384, 387, 942, and 945. The 1,2,3-guanidinium group of STX may interact with the carboxyl at position 1717 of repeat IV, which has much less influence on TTX block (Table 1). We propose that three of the carboxyls of repeats I and II interact with the guanidinium group, while the fourth negatively charged residue forms two hydrogen bonds with neighboring hydroxyl groups of C9 and C10 for TTX and C12 for STX. Among the four carboxyl sites Glu^{945} appears to be less important for TTX binding than the others, since the mutation E945Q reduces TTX sensitivity less than the other mutations. Most probably, Glu^{945} interacts with the TTX hydroxyls. Indeed, the hydrogen bond formed by the C10-OH group is rather weak, as indicated by its easy deprotonization (Kao, 1986). On the other hand, both hydrogen bonds formed by the gem-diol group of STX are strong, so that Glu^{945} is as important as the other carboxyls for STX binding (Kontis and Goldin, 1993). It seems plausible that Glu^{945} interacts with the toxin hydroxyls, and the other three carboxyls at positions 384, 387, and 942 form ion-pair salt bridges with the guanidinium group.

We will consider an arrangement for toxin binding that includes four loci for TTX and five loci for STX (Fig. 1). This scheme is in accordance with the three resonance forms of the guanidinium, in which the positive charge is distributed between the N—H groups. Moreover, there are examples in proteins where different N—H groups of Arg form salt bridges with some carboxyl groups of Asp or Glu (Proegman et al., 1978). Consequently, each of the three carboxyl residues would contribute almost equally to interaction with the guanidinium group, and the fourth carboxyl group gives approximately similar energetic contribution. Fersht et al. (1985) showed that the energy of a salt bridge is approximately equal to that of two neutral hydrogen bonds.

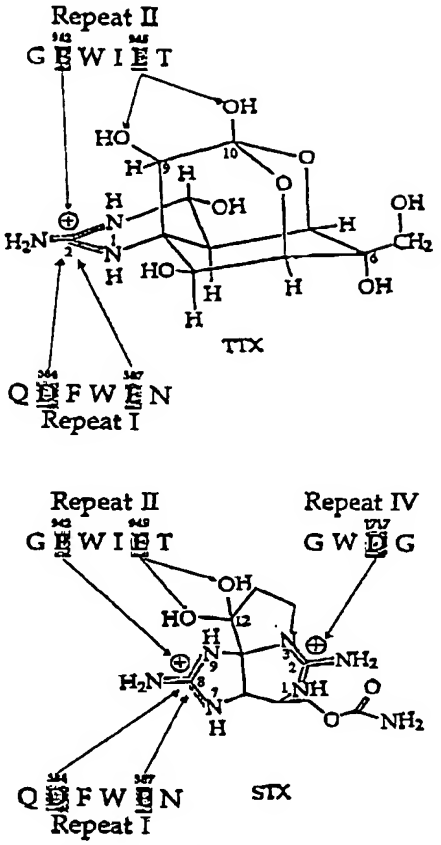

FIGURE 1 Molecular structures of TTX and STX and suggested amino acid interactions of the Na^+ channel (see Fig. 2). There are four loci for TTX and five loci for STX. The toxin structures are from Hille (1992).

Conformation of the SS1 and SS2 peptide fragments

The first step in predicting a satisfactory protein structure for toxin interaction was to examine the probable structural properties of the peptide chains comprising the SS1 and SS2 segments from the four repeats of rBrII (Fig. 2), taking into

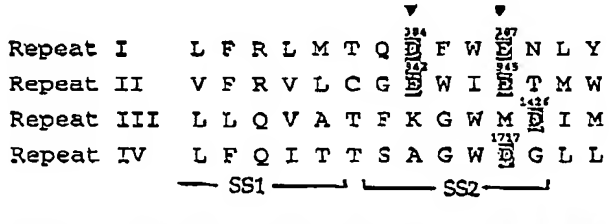

FIGURE 2 The SS1-SS2 regions (P-loops) of repeats I–IV of the rat brain II Na^+ channel. Positions of certain critical mutations are marked (from Terlau et al. (1991)).

account the probably extracellular location of these segments. SS1 and SS2 contain many residues that have high probability for appearance in β-strands or β-structures: Val, Ile, Tyr, Cys, Trp, Phe, Thr, Met, and Leu (Creighton, 1993). For example, in the case of the SS1 fragment of repeat II there are five bulky hydrophobic residues in the C-terminal six-member segment: Ile, Val, Leu, and Phe (Fig. 2). On the other hand, residues at the border between SS1 and SS2 have a conformational preference to participate in reverse β-turns: Gly, Asp, Ser, and Lys (Wilmot and Thornton, 1988). Therefore, this region has a high probability to form β-hairpins, in which adjacent β-strands are linked through β-turns and produce a structure that might exist at an interface between the hydrophilic surface and the hydrophobic core or the protein.

In order to select likely positions for the β-turns in the peptide chains we used the procedure proposed by Chou and Fasman (1978), but taking into account newer values for the conformational preferences (P_t) found on the basis of x-ray data of proteins (Williams et al., 1987). The values of P_t characterize the relative tendencies of residues to be involved in β-turns (Table 2). Values of $P_t > 1.0$ characterize amino acid residues favoring β-turns. According to Chou and Fasman (1978), a β-turn is predicted if a four-residue sequence has an average value $\langle P_t \rangle > 1$ (and $\langle P_t \rangle > \langle P_\beta \rangle$). Further, values of P_t for the two central residues of the β-turn should be greater than those for the extreme residues. These conditions are reasonably met on the central portions of the four peptide fragments underlined in Table 2 ($\langle P_t \rangle$ = 0.96, 0.99, 1.02, and 1.12, respectively). The sequences preceding the proposed β-turns are composed of residues with low probability of participating in turns. For repeat IV a second possible turn region is seen, but we selected the first one for reasons presented later. In this manner, we chose the four β-hairpins of repeats I–IV, composed of two β-strands connected in the center by β-turns (as marked in Table 2), and consisting of 10 residues each. It was important to include all of the SS2 amino acids, in order to stabilize the β-hairpin. The 1–2 adjacent residues on both ends also have a high probability of being in β-strands, and the usual length of such β-hairpins is 8–16 amino acids (Sibanda et al., 1989). Since these are no longer identical with the original definition of the SS1 and SS2 segments, we will call them beta1 and beta2 on the N and C ends, respectively.

The conformations of the β-hairpins are important for our modelled structure, because they determine the characteristic orientation of side chains (Fig. 3). We adopted the usual numbering for the four residues that comprise β-turns (i, $i + 1$, $i + 2$, and $i + 3$) (Creighton, 1993). Neighboring residues of the β-strands alternate relative to the plane of the β-hairpin (up-down-up...). Residues i and $i + 3$ belong to both the β-turn and the β-strand. If residues $i + 2$, $i + 3$, and $i + 5$ of beta2 are located on the outside plane of the β-hairpin, the residues $i + 1$, $i + 4$, and $i + 6$ are found on the opposite side. In repeat I we know from mutation studies that Asp^{384} ($i + 2$) is important for toxin block. Therefore, Phe^{385} ($i + 3$), and Glu^{387} ($i + 5$) would be important for toxin block, also consistent with mutation data, and other residues of the fragment that face away from the toxin site would be relatively unimportant. In like manner we can predict for repeat II that only residues in positions $i + 2$, $i + 3$, and $i + 5$ (Glu^{942}, Trp^{943}, and Glu^{945}) have the correct location to interact with toxin. Effects of these residues would be large (two to four orders of magnitude), while other residues would produce only small effects on toxin interaction by secondary changes in the binding structure.

TTX interacted with primarily the segments of repeats I and II. These two repeats can be aligned to form a structure consisting of two antiparallel β-hairpins adjacent to each other. This structure produces a cavity for binding of TTX, with the inner part consisting of six side chains of residues Asp^{384}, Phe^{385}, Glu^{387}, Glu^{942}, Trp^{943}, and Glu^{945} (Fig. 4). Presumably the β-hairpins of repeats III and IV form mainly the outer walls of the binding cavity for TTX, with the β-hairpins also arranged in an antiparallel fashion. For repeat III this results in the possibility of toxin interaction with the residues of Lys^{1422} ($i + 1$), Met^{1425} ($i + 4$), and Ile^{1427} ($i + 6$). The residues of interest for repeat IV in the arrangement are Ala^{1714} ($i + 1$), Asp^{1717} ($i + 4$), and Leu^{1719} ($i + 6$). Indeed, alignment of the β-hairpin of repeat IV in an antiparallel relationship to that of repeat I on the front wall changes the directions of its side chains in space, so that the side chains of residues $i + 1$, $i + 4$, and $i + 6$ are inside the

TABLE 2 Conformational preferences P_t* for residues in SS1–SS2 segments of the muscle channel and positions of β-turns (*underlined*)

								384			387		
Repeat I	L	F	R	L	M	T	Q	D	Y	W	E	N	L
P_t	0.57	0.59	0.90	0.57	0.52	0.90	0.84	1.24	0.86	0.65	1.01	1.34	0.57
								942			945		
Repeat II	V	F	R	V	L	C	G	E	W	I	E	T	M
P_t	0.41	0.59	0.90	0.41	0.57	0.54	1.77	1.01	0.65	0.47	1.01	0.90	0.52
								1422			1425		
Repeat III	L	L	Q	V	A	T	F	K	G	W	M	D	I
P_t	0.57	0.57	0.84	0.41	0.82	0.90	0.59	1.07	1.77	0.65	0.52	1.24	0.47
								1714			1717		
Repeat IV	L	F	Q	I	T	T	S	A	G	W	D	G	L
P_t	0.57	0.59	0.84	0.47	0.90	0.90	1.22	0.82	1.77	0.65	1.24	1.77	0.57

* From Williams et al. (1987).

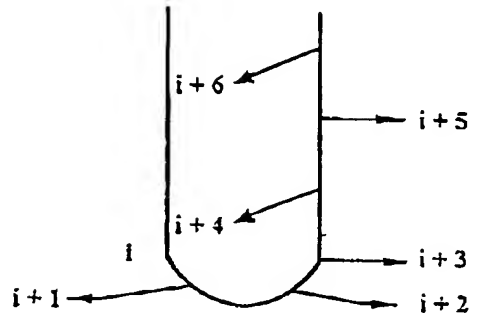

FIGURE 3 Directions of side chains in the β-hairpins. The residues in the β-turns are numbered i to $i + 3$.

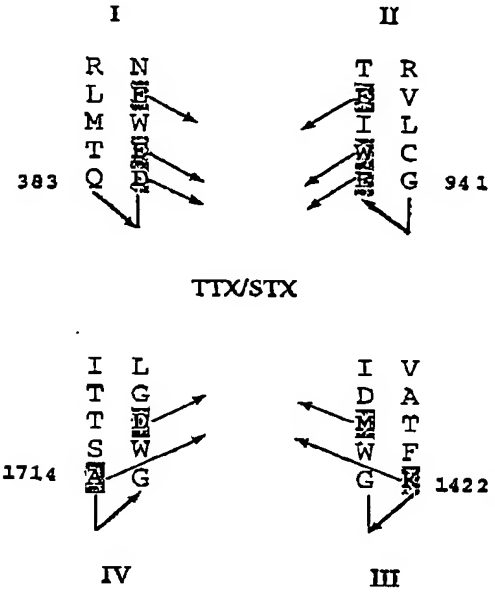

FIGURE 4 Structural motif for the TTX/STX binding site of the Na^+ channel—an antiparallel arrangement of β-hairpins of repeats I–IV. Residues that interact with toxins are marked by arrows. The numbered residues are located in positions $i + 1$ of β-turns. Relative orientation of β-turns of the four hairpins is shown by flat arrows connecting the beta1 and beta2 strands, and it corresponds to an overhead view.

binding cavity. In this model the residues at $i + 6$ can be ignored, because they are above the level of the toxin molecule. This structural motif of the toxin binding site forms a funnel-like aggregate barrel, consisting of four antiparallel β-hairpins with the beta2 strands facing the vestibule and the beta1 strands on the outside toward the protein core (Fig. 4).

Comparison of the structural motif to mutation data

The arrangement of the four β-hairpins into an antiparallel structure results in a vestibule-like cavity appropriately sized for a toxin binding pocket. Although some of the mutation data were used to make our initial selection of interactive sites, model predicts correctly the results of mutation of all of the residues reported by Terlau et al. (1991). Neutralization of the aspartic and glutamic acid residues (but not swapping these residues) at positions $i + 2$ and $i + 5$ of repeat I and $i + 2$ of repeat II resulted in loss of both TTX and STX block (Table 1). Neutralization of glutamic acid at position $i + 5$ of repeat II greatly reduces toxin block, similar to the effect of toxin analogs that affect the hydroxyl sites. The model also predicts possible participation of the residue at positions $i + 3$ in repeat I. Satin et al. (1992) demonstrated that substitution of Phe^{385} or Tyr in place of the naturally occurring Cys resulted in an increase in TTX and STX affinity of about 1000 ×. Backx et al. (1992) found that the reverse mutation of tyrosine to cysteine in the skeletal isoform reduced toxin affinity dramatically, and Heinemann et al. (1992a) demonstrated the same effect for mutation of phenylalanine to cysteine in rBrII. Terlau et al. (1991) reported mutations in repeats I and II in positions $i + 1$ (Q383E, Q383K, G941E) and $i + 6$ (N388R) that had less than 10-fold effects on toxin block. The W386C mutation at $i + 4$, which reduced TTX block 30-fold (Tomaselli et al., 1993), is a very nonconservative change, and it undoubtedly caused some structural reorganization of the vestibule. Mutations beyond the 10 amino acid β-hairpins modelled here (R379Q, Q391K, D949N, E952Q) had little effect (Terlau et al., 1991; Kontis and Goldin, 1993), suggesting that the dimensions of the proposed vestibule are appropriate.

The mutants of residue Asp^{1426} in repeat III and of residue Asp^{1717} in repeat IV represent a good test of the antiparallel alignment of the β-hairpins. This model predicts that side chains in position $i + 5$ of repeats III and IV are directed outside the pocket. Indeed, mutants of this carboxyl of repeat III (D1426N, D1426Q, D1426K) do not affect toxin block significantly (Table 1). On the other hand, substitution by a positive charge at position $i + 4$ of repeat III did interfere with block of both toxins (M1425K). In repeat IV position $i + 4$ is active, and all three mutants of Asp^{1717}—D1717N, D1717Q, and D1717K do not bind STX. Besides, the residue at position $i + 1$ can influence toxin block (A1714E). In summary, the structural model we propose is consistent with the toxin sensitivity of the mutants of the SS1-SS2 peptides so far reported.

ENERGETIC IMPLICATIONS OF THE TOXIN BINDING POCKET

Molecular modelling

Modelling was accomplished in the Insight and Discover graphical environments (Biosym Technologies, Inc., San Diego). The molecular mechanics energetic calculations utilized the force field cvff (consistent valence force field), which was specifically derived to fit structures of peptides and proteins. In this approximation the formation of hydrogen bonds is modelled as an electrostatic interaction. For minimization procedures the steepest descents and conjugate gradients have been used.

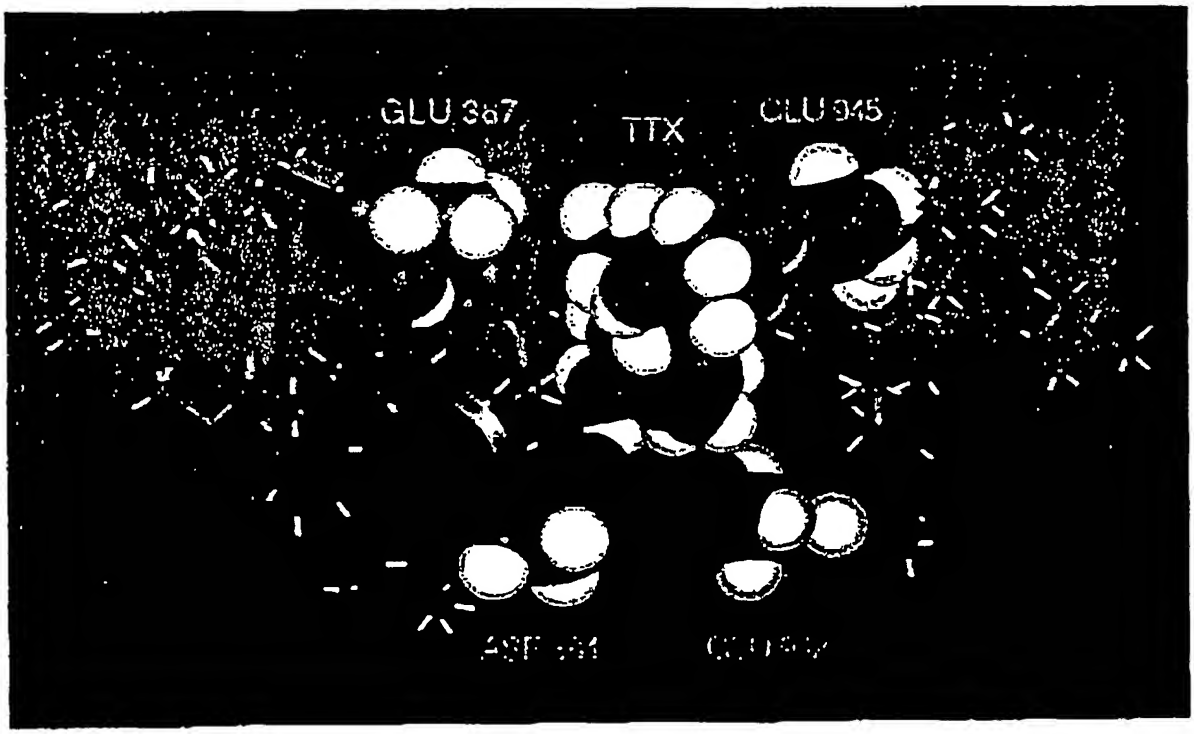

FIGURE 5 Spatial model of the complex of TTX with the beta1 and beta2 strands of repeats I and II of the cardiac Na^+ channel isoform. Four critical carboxyl residues and the TTX are identified as space-filling images, while the remainder of the β-hairpins are shown with a backbone ribbon and stick side chains.

Modelling of the outer vestibule of the Na^+ channel was accomplished in three stages. First, the optimal conformations of the β-hairpins were calculated. Second, the interaction of TTX with the repeat I and II peptides were obtained. The peptides of repeats III and IV were assumed to form only the remaining walls of the pocket. Finally, STX was substituted into the repeat I–II structure derived from interaction with TTX and repeats III and IV were added. The optimal spatial structures of TTX and STX were determined in the same program environment on the basis of their chemical structures and specific configurations (Kao, 1986).

The reasons for modelling the decapeptide of each repeat as a β-hairpin have been discussed, but each residue conformation must be determined. In this structure the two β-strands are united by a β-turn. As zero approximation for angles of rotation $\phi(C^\alpha - N)$ and $\psi(C^\alpha - C')$ in the backbone of the peptide chain of β-strands the angles of rotation in standard antiparallel β-structure, $\phi(C^\alpha - N) = -139°$ and $\psi(C^\alpha - C') = +135°$ (Creighton, 1993) have been taken, while for the two central residues of the β-turns with numbers $i + 1$ and $i + 2$ we used angles of rotation in reverse β-turns of type III: $\phi(C^\alpha - N) = -60°$ and $\psi(C^\alpha - C') = -30°$ (Wilmot and Thornton, 1988). Angles ϕ and ψ in β-strands correspond to region B of conformational maps $\phi - \psi$ ($\phi < 0°$, $\psi > 0°$), while the angles ϕ and ψ in β-turns of type III correspond to region R ($\phi < 0°$, $\psi < 0°$). Therefore we note the corresponding conformational states of the amino acid residues by the symbols B and R.

As a preliminary step during the search for optimal conformation of the β-hairpins of repeats I and II, minimization of potential energy of the pentapeptide fragments on the N and C ends in the conformations BBBBR and RBBBB was carried out. Since only the C ends of the two β-hairpins (the beta2 strands) interact directly with TTX, we found the optimal conformations of repeat I (Asp-Cys-Trp-Glu-Arg (for the cardiac channel), Asp-Tyr-Trp-Glu-Asn (for the muscle channel), and Asp-Phe-Trp-Glu-Asn (for the rat brainII channel)) and of repeat II (Glu-Trp-Ile-Glu-Thr). These pentapeptides were allowed to interact with TTX and new approximations of the angles of rotation $\chi_1(C^\alpha - C^\beta)$, $\chi_2(C^\beta - C^\gamma)$ were obtained for the side chains of residues of Asp and Glu such that they were in maximal proximity to the guanidinium group of TTX. It was possible only when fragments Asp-*X*-*X*-Glu and Glu-*X*-*X*-Glu accepted the conformation RBBB; that is, the conformation of the beta2 strands. After minimization of the energies of these complexes the carboxyl groups of the side chains of Asp and Glu formed optimal hydrogen bonds with the guanidinium group of TTX.

The optimal conformations of the BBBBR fragments of the N ends and the complex conformations derived above for RBBBB of the C ends of the β-hairpins were used to form the two decapeptide β-hairpins of repeats I and II in the

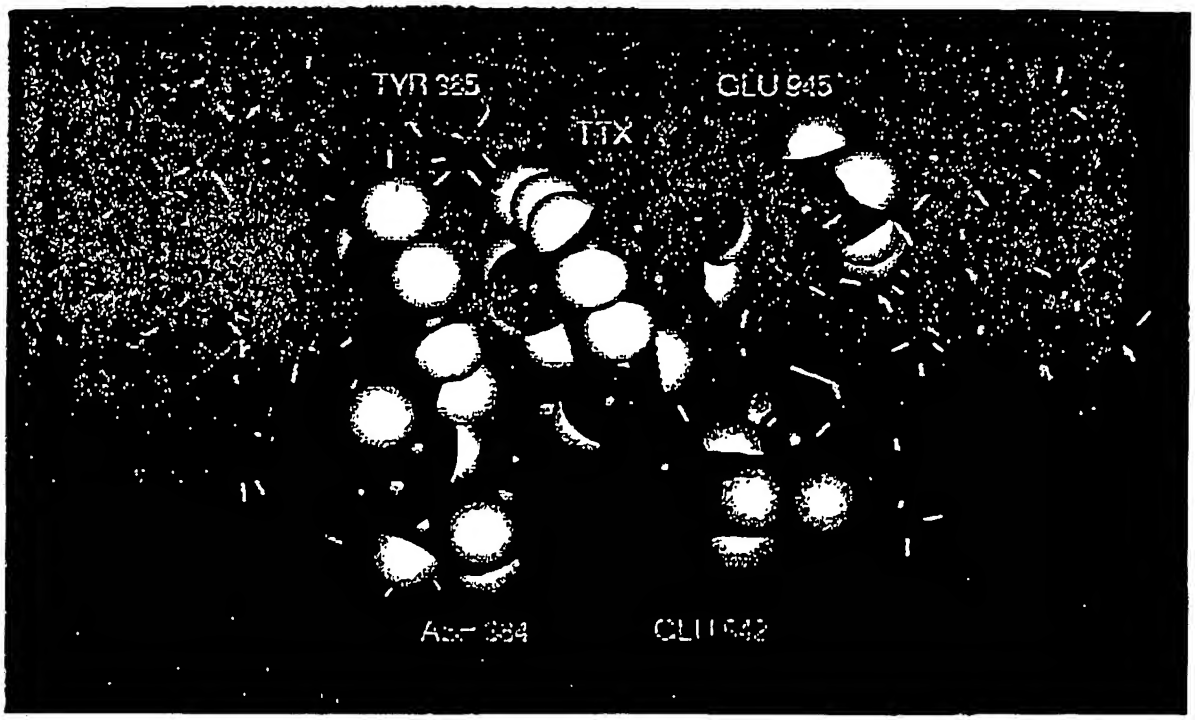

FIGURE 6 Spatial model of the complex of TTX with the beta1 and beta2 strands of repeats I and II of the adult skeletal muscle isoform of the Na^+ channel. The residue Tyr^{385} is also shown in a space-filling image. Note the proximity of the aromatic ring of Tyr to the hydrophobic surface of the TTX.

conformation BBBBRRBBBB. For angles of rotation ϕ and ψ in residues $i + 1$ and $i + 2$ in the β-turns the initial condition that there was a hydrogen bond C═O ··· H—N between residues i and $i + 3$ in the chain was used.

Finally, the three part structure of β-hairpins of repeats I and II and TTX was obtained by combining the TTX molecule in its complexes with the β-hairpins of both repeats I and II for energy minimization of the ensemble. This resulting complex is shown for the cardiac isoform in Fig. 5. The two β-hairpins of repeats I and II form a cavity with the dimensions of TTX. The depth of the cavity is 12–13 Å. The bottom is formed by two carboxyl groups of the side chains of Asp^{384} and Glu^{942} in their $i + 2$ positions on the two β-turns. The distance between the closest oxygens is 4.7 Å, providing room for water molecules in between for compensation of electrostatic repulsion. The distance between the outer carboxyls of Glu^{387} and Glu^{945} are significantly larger at 8.1 Å, so that they could not form direct hydrogen bonds with each other. The back wall of this cavity is formed by the side chain of Trp^{943} of repeat II. As described before, three carboxyls simultaneously form salt bridges with the guanidinium group (Glu^{387} with N(1)—H, Asp^{384} with N(2)—H, and Glu^{942} with N(3)—H), while Glu^{945} forms two optimal hydrogen bonds with the two hydroxyl groups C9-OH and C10-OH of TTX (Fig. 5). The distance between oxygens of the carboxyls and protons of the corresponding N—H groups of TTX in this complex are 2.4–2.6 Å. These distances are slightly greater than the corresponding distances in complexes of TTX with individual chains of repeats I or II (2.1–2.2 Å). In the three part complex the salt bridges have slightly less energy than with only one repeat and TTX. On the other hand, the distances O ··· O in hydrogen bonds formed by side chains of Glu^{945} with C9-OH and C10-OH groups are 3.0 Å, corresponding to optimal hydrogen bonds OH ··· O ((O ··· O) = 2.8 ± 0.1 Å (Pimentel and McClellan, 1960)).

Calculation of the energy of interaction

Nonbonded and electrostatic interactions were calculated. For the complex of repeats I and II and TTX for the cardiac isoform, energies of nonbonded interactions with residues 384, 385, 387, 942, and 945 (rBrII numbering) were −1.5 to −2 kcal/mol, although Trp^{943} had an energy of −4.8 kcal/mol. Electrostatic interactions were calculated using a dielectric constant $\epsilon = 10$, appropriate to calculations for peptide chains in polar (water) media (Krimm and Mark, 1968). Energies of electrostatic interactions for each of the glutamic and aspartic acids, including Glu^{945} with two hydrogen bonds to C9-OH and C10-OH is about −7 kcal/mol. In addition to these, there is electrostatic interaction with the positive side chains of Arg (378, 388, and 937), although there are no nonbonded interactions with them. Therefore, the total of nonbonded and electrostatic interactions of TTX with the β-hairpins of repeats I and II of the cardiac isoform are calculated to be −15.6 and −18.2 kcal/mol, respectively.

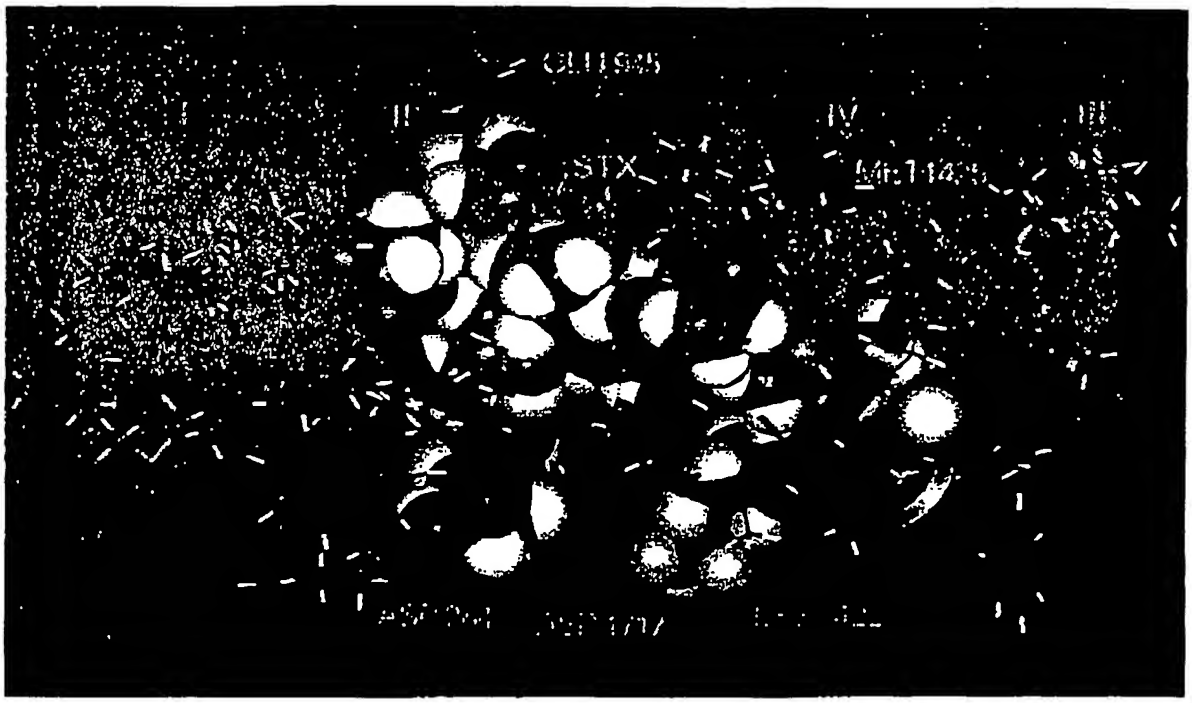

FIGURE 7 Spatial model of the complex of STX with the beta1 and beta2 strands of repeats I–IV of the cardiac Na^+ channel isoform. Note the proximity of the second guanidinium group and carbamyl of STX in the center of the model to Asp^{1717} of repeat IV.

The above calculations were made for the cardiac isoform so that we could compare the model to the experimental results of Satin et al. (1992). They reported that substitution of a Tyr or Phe for Cys^{385} increased the sensitivity of TTX block about 1000 times. This suggests that there is an important nonpolar interaction with TTX. Indeed, TTX has asymmetrical distribution of -OH groups. The surface opposite to the C9 and C10 hydroxyls contains mainly protons of C—H groups. Replacement of the Cys^{385} with either Tyr or Phe causes the aromatic rings to be parallel to the nonpolar surface of TTX (Fig. 6). The nonbonded energy of interaction for tyrosine or phenylalanine is −7 kcal/mol, while that for cysteine is only −2.1 kcal/mol, and energetic gain of about 5 kcal/mol for interaction with the repeat I β-hairpin, as suggested by Satin et al. (1992), and generally supports the structural motif.

The 7,8,9-guanidinium group of STX forms the same physical relationship and energy of interaction as that of the TTX guanidinium group. As before, this group takes part in the same salt bridges with Asp^{384}, Glu^{387}, and Glu^{942}. The interaction of Glu^{945} with two hydroxyls is preserved by the two hydroxyls at C12 of STX. After energy minimization of the three element complex, optimal hydrogen bonds were formed with O ··· O distances of 3.0 Å. It is apparent that STX shares the same sites as TTX on repeats I and II, in accordance with the close agreement with their biological action (Kao, 1986). The nonbonded interaction energies are almost identical. However, the second 1,2,3-guanidinium group influences the electrostatic interactions in two ways. The energies of electrostatic interaction of STX with the side chains of Asp and Glu (384, 387, 942, and 945) are larger in absolute scale that those for TTX, but this is compensated by repulsion of the Arg interactions. Consequently, the energies of binding of TTX and STX with the two β-hairpins of repeats I and II are almost identical.

The other two β-hairpins of repeats III and IV were aligned by allowing a salt bridge between the 1,2,3-guanidinium group of STX and the side chain of Asp^{1717} of repeat IV and the presence of van der Waals contacts between STX and the side chain of Met^{1425} of repeat III. Neutralization of Asp^{1717} (D1717N) reduced STX block. Substitution of Gln for Met^{1425} had little effect, but its replacement by the positively charged Lys prevented block (Terlau et al., 1991). We interpret this to mean that the side chain of Met has a nonbonded interaction with STX. Finally, the complex of STX and the four β-hairpins of repeats I–IV was evaluated, including dense packing of β-hairpins but omitting van der Waals repulsions of their neighboring side chains (Fig. 7). In this structure two protons at N(2) of the 1,2,3-guanidinium group form hydrogen bonds with the carboxyl of Asp^{1717}, and the carbamoyl group of STX also takes part in effective electrostatic interactions with this residue of repeat IV. Altogether, the energy of nonbonded and electrostatic interactions of STX with the β-hairpin of repeat IV is −13 kcal/mol. The energy of interaction of STX with the β-hairpin of repeat III is significantly smaller: −1.4 kcal/mol. The Cartesian co-

TABLE 3 Cartesian coordinates (Å) of some groups in the complex of STX with repeats I–IV (World scale system of Insight II)

	Atom	X	Y	Z
Residue				
Repeat I				
Asp^{384}	C^{γ}	16.23	0.86	−5.25
	O	16.09	2.09	−5.40
	O	15.02	0.07	−5.51
Glu^{387}	C^{δ}	12.32	−1.33	−12.01
	O	13.97	−0.79	−12.05
	O	12.10	−1.34	−10.91
Repeat II				
Glu^{942}	C^{δ}	13.10	3.95	−3.11
	O	12.82	2.78	−3.55
	O	14.25	4.42	−3.15
Glu^{945}	C^{δ}	5.52	0.19	−7.22
	O	6.73	0.11	−6.93
	O	4.86	−0.81	−7.57
Repeat III				
Met^{1425}	S^{δ}	11.17	−7.37	0.49
	C^{ϵ}	11.66	−5.64	0.37
	H	11.94	−5.37	−0.66
	H	10.83	−4.98	0.69
	H	12.53	−5.44	1.03
Repeat IV				
Asp^{1717}	C^{γ}	13.61	−8.02	−5.48
	O	13.26	−6.87	−5.24
	O	13.99	−8.47	−6.71
Group of STX				
7,8,9-Guanidinium	N7	11.31	−0.66	−7.70
	H	11.18	−0.49	−8.81
	C8	12.07	0.18	−6.88
	N8	12.78	1.20	−7.33
	H	12.76	1.37	−8.34
	H	13.30	1.75	−6.63
	N9	12.10	−0.19	−5.53
	H	12.56	0.57	−4.81
$C12-(OH)_2$	C12	9.64	−0.66	−4.76
	O	8.51	−1.51	−5.01
	H	7.83	−0.94	−5.39
	O	9.29	0.64	−5.22
	H	8.65	0.52	−5.93
1,2,3-Guanidinium	N1	11.90	−4.01	−6.06
	H	12.16	−4.99	−6.19
	C2	11.75	−3.58	−4.68
	N2	12.05	−4.48	−3.75
	H	12.37	−5.40	−4.07
	H	11.93	−4.18	−2.77
	N3	11.26	−2.23	−4.35

ordinates of some of the important groups of this complex are given in Table 3.

The difference in energy of interaction between STX and TTX was estimated by substituting TTX for STX in the four β-hairpin model. The nonbonded interaction energies with repeats III and IV are the same, but the loss of the additional electrostatic energy of the 1,2,3-guanidinium group reduced the TTX interaction energy by 6 kcal/mol, giving it a lower affinity than STX. We did not calculate free energy of these interactions, so these values cannot be directly converted into binding affinities for experimental comparison. However, the calculated energy differences between isoforms and between toxins are experimentally consistent.

Although the proposed model of the Na^+ channel vestibule as the toxin binding pocket fits the mutation data presently available, there are several uncertainties to be considered. First, the outside of the pocket faces other parts of the protein, which could have significant effect on the shape and stability of the β-hairpin region. Second, the activities of water and protons in the vestibule could be restricted, affecting the electrostatic interaction energies and the local pH. Finally, the effects of such mutations as K1422E and A1714E (Terlau et al., 1991) do not mean that in native channels Lys and Ala interact with the toxins, because the addition of carboxyls at these sites may create new loci for toxin interaction.

β-TURNS OF THE TOXIN BINDING POCKET FORM THE ION SELECTIVITY FILTER

The mutation studies of Terlau et al. (1991) included estimates of the single channel conductances from noise analysis. Although many of the mutations had no effect on single channel conductance, neutralization of the glutamic acid or aspartic acid residues reduced it. Specifically, neutralization of Asp^{384} (D384N) and Glu^{942} (E942Q) greatly reduced ionic current (Table 1). These residues are located in positions $i + 2$ of β-turns of repeats I and II, and they are apparently involved both in toxin binding and ion conduction of the Na^+ channel. Subsequent studies by Heinemann et al. (1992b) showed that simultaneous mutations of two residues in repeats III and IV (K1422E and A1714E) made the Na^+ channel permeable to Ca^{2+}. They suggested that the resulting four negatively charged side chains at positions 384, 942, 1422, and 1714 reproduce the structure of the selectivity filter of Ca^{2+} channels. Such a change in selectivity is in accordance with our structural model, because the two mutations refer to residues at positions $i + 1$ of the β-turns of repeats III and IV, which because of this antiparallel arrangement are directed to the inside of the binding cavity (Fig. 8). It is interesting to consider the hypothesis that two carboxyls at this site are responsible for Na^+ selectivity of the native Na^+ channel, but that three or four are required for Ca^{2+} permeation.

The ions Na^+ and Ca^{2+} have the same ionic radii (1.02 and 1.00 Å) in crystallohydrates. They are typically octahedrally coordinated with six molecules of water, but because of the difference in charge, they have very different hydration energies (−105 kcal/mole for Na^+ and −397 kcal/mole for Ca^{2+}) (Hille, 1992). This leads to the idea that electrostatic interaction of Na^+ with the two carboxyls at positions 384 and 942 are able to reduce the hydration shell energy sufficient to decrease the barrier to Na^+ movement through the channel pore. However, three carboxyls may be required for weakening of the hydration shell of Ca^{2+}. Three are suggested because the single mutant K1422E and the double mutant K1422E and A1714E have the same Ca^{2+} conductance (Heinemann et al., 1992), so that only the carboxyl at position 1422 may be involved.

In the four β-hairpin model of the Na^+ channel with the toxin removed, Na^+ coordinates with Asp^{384} and Glu^{942} to force out two or more molecules of water. Coordination of

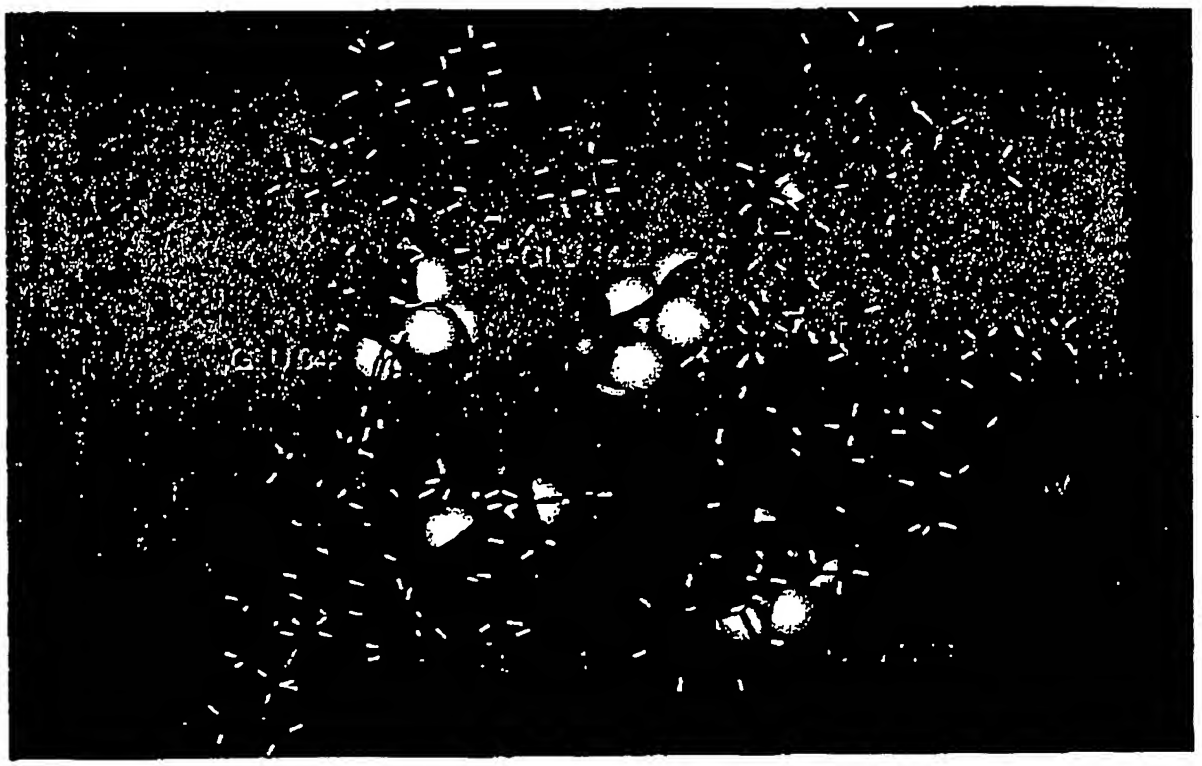

FIGURE 8 Double mutant of the toxin binding site of the Na^+ channel structure with toxin removed (K1422E and A1714E (Heinemann et al., 1992b)).

$Na^+ \cdot 4H_2O$ in this region, which weakens binding energy between Na^+ and water in the transition state is shown in Fig. 9. For the double mutant K1422E and A1714E (Fig. 8), the carboxyls of three side chains (Asp^{384}, Glu^{942}, and Glu^{1422}) can be coordinated with $Ca^{2+} \cdot 3H_2O$, substituting for three molecules of hydration water. In the double mutant model Glu^{1714} does not coordinate with Ca^{2+} because of the asymmetrical structure of this region. This region of the model is similar in size to that suggested by Hille (1971) for the dimensions of the Na^+ channel selectivity filter (3.1 × 5.1 Å). Evidently, selectivity filters in Na^+ and Ca^{2+} channels promote the formation of ions with only one molecule of water ($Na^+ \cdot H_2O$ and $Ca^{2+} \cdot H_2O$), which then pass through the channel pore.

DISCUSSION

The purpose of the model was twofold. Firstly, we wished to determine if the recently available mutation data from cloned Na^+ channels, in combination with the structures of the toxins and their analogs, would lead to a structurally satisfactory toxin binding site. Secondly, defining the site would characterize the structure of part of the permeation path, if the toxin binding site is in the path. Most investigators have assumed that the toxins block by physically occluding the channel, (Hille, 1975; Strichartz, 1984; Kao, 1986). However, Green et al. (1987) have offered biophysical evidence that the toxin binding site is at a distance from the permeation path. The mutation studies of Terlau et al. (1991), Satin et al. (1992), Backx et al. (1992), and Kontis and Goldin (1993) identified several amino acids in the SS1-SS2 regions of each of the four Na^+ channel repeats as critical for toxin binding. Further, Terlau et al. (1991) and Heinemann et al. (1992b) showed that mutations of several of these amino acids change single channel conductance and selectivity of the channel. This demonstration of structural overlap of the toxin binding site and the conductance/selectivity region is strong evidence that the toxin site is indeed in the permeation path.

The proposed model is supported by appropriate interactions with amino acid residues identified by mutation studies and by consistency with the interaction of various toxin analogs. It provides a rationale for differences in binding between TTX, which interacts directly with the SS1-SS2 segments of repeats I and II, and that of STX, which additionally interacts with the segments of repeats III and IV. It also provides a basis for predicting the blocking affinity of new analogs and the effects of other mutations in the binding region. This is illustrated by the model prediction that the differences in toxin binding between the brain/skeletal and the cardiac isoforms is the result of a hydrophobic interaction with the aromatic rings of Phe or Tyr, while Cys may be a spacer element that interacts only weakly.

An unexpected but welcomed outcome of the model was its prediction of the narrow region delineated by residues of

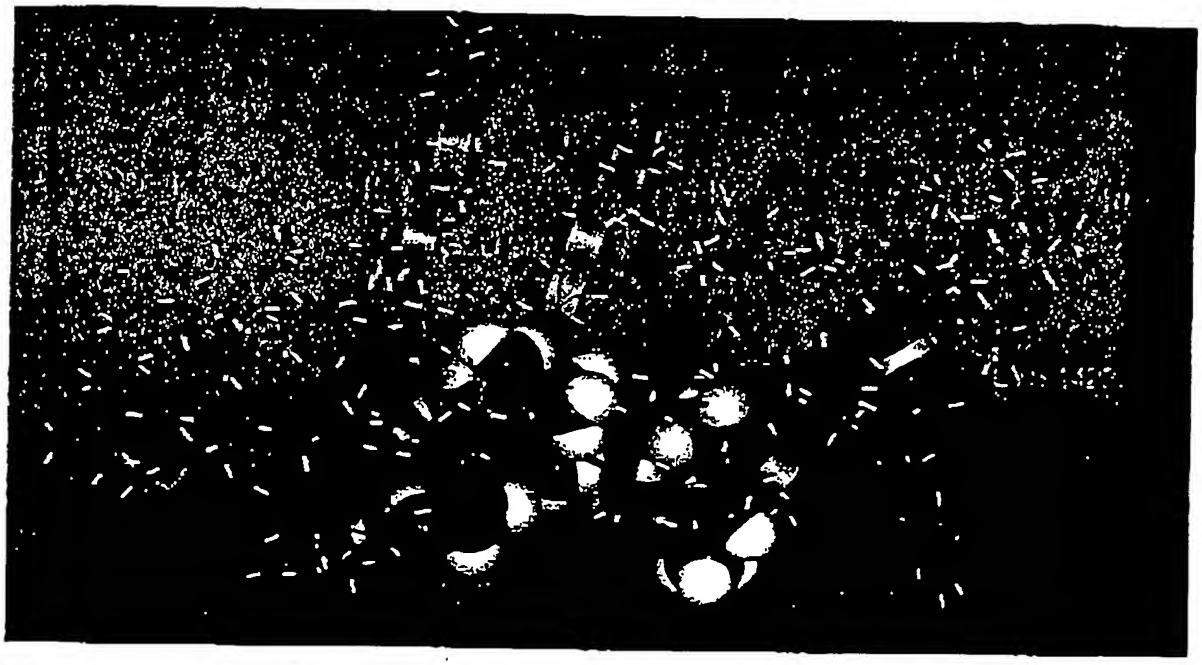

FIGURE 9 Coordination of the hydrated Na^+ ion (Na^+-$4H_2O$) with the carboxyls of Asp^{384} and Glu^{942} of the cardiac isoform. Na^+ is in violet. The carboxyls substitute for two of the waters of hydration in the transition state.

the β-turns of the four β-hairpins (384, 942, 1422, 1714). This region has been proposed as a candidate for the selectivity filter by Heinemann et al. (1992b) on the basis of mutation studies. When the toxin was removed from the model pocket formed by the four β-hairpins, the narrow region at the turn points had dimensions close to those predicted by Hille (1971, 1992) on the basis of permeation of organic molecules of various sizes and shapes. Assuming that the molecule is stabilized in this conformation by the rest of the underlying protein, the carboxyl residues at positions 384 and 942 on repeats I and II were located correctly for interaction with the hydrated Na^+ ion ($Na{\cdot}6H_2O$), displacing two water molecules and reducing the energy of interaction of the other waters of hydration. However, a third carboxyl on repeat III, shown by Heinemann et al. (1992b) by mutation studies to produce a channel with significant Ca^{2+} permeation, was correctly located in the putative selectivity region to provide an additional displacement of a third water molecule in its hydration shell and decrease the energy of hydration of the other water molecules. We consequently support the suggestion that this region may represent the channel's selectivity filter. Moreover, substitution of either Glu334 or Glu1086 by Lys in the homologous selectivity positions in the human cardiac Ca^{2+} channel α1-subunit leads to a significant increase in Na^+ permeation through the Ca^{2+} channel (Tang et al., 1993). Indeed, according to our model, the spatial arrangement of carboxyls of pairs of glutamic acids 334 and 677 or 677 and 1086, which are necessary for Na^+ permeation of the Ca^{2+} channel is approximately the same as in the triangle of residues 384, 392, and 1422 of the Na^+ channel (Fig. 8).

The appropriate location of the residues of repeat III for simulation of a Ca^{2+} coordination site was the consequence of the antiparallel alignment of the β-hairpins. This does not conflict with possible pseudo 4-fold symmetrical arrangement of the transmembrane segments S1–S6 of repeats I–IV, because the lengths of the segments connecting beta2 to S6 are different. In the case of repeats I and II, they are 9 residues each, whereas for repeats III and IV, they are 19 and 30, respectively, and consequently could accommodate additional loops in repeats III and IV.

Another outcome of the model is the prediction of the structure of the outer vestibule of the channel, defined as the region large enough to accommodate the bulky toxin molecules. The size of this putative vestibule and the location of charged residues are consistent with the modelling studies of Dani (1986) and Cai and Jordan (1990). They provide specific dimensions for future modelling and predictions of the outcomes of mutation studies on surface charge phenomena. This model also allows consideration of interactions between the channel and peptide toxins such as μ-conotoxin, which competes with TTX and STX in blockade of the adult skeletal muscle and eel electroplax channel isoforms (Becker et al., 1992).

In this model the peptide fragments beta1 and beta2 of the P region create only the outer vestibule of the Na^+ channel, with the selectivity filter at its bottom. These peptides do not form the remainder of the transmembrane pore, in contrast

to some previous models of Na^+ and K^+ channels. A simple examination of the P regions shows that the amino acid composition is very different, with many charged residues in the Na^+ channel mouth. Consequently, it is likely that there will be significant differences in the structures of the pore regions of the two channel types.

An important but unresolved question is the possible presence of an electric field in this vestibule and its effect on toxin binding. Schild and Moczydlowski (1991), Satin et al. (1992), Backx et al. (1992), and Doyle et al. (1993) identify a site for divalent ion block within the electric field. Because divalent ion binding is competitive with toxin binding, this implies that there is a field drop within this structural element and predicts that toxin binding should show some voltage dependence.

Although the proposed model is effective in its prediction of isoform/mutation and toxin analog studies, the interface of these four β-hairpins with the rest of the protein could not be considered. It should be clear that such interactions would be important for the shape and stability of the vestibule. The model does provide a basis for selecting other mutations of these peptide segments, which could result in structural refinement, particularly with regard to the mechanism of selectivity.

We thank David Piper for his assistance in the computer simulations, and Dr. Dorothy Hanck for productive discussion during the course of this work. This work was supported in part by PO1-HL20592, the Sprague Memorial Foundation, and the University of Chicago Cardiology Molecular Modelling Core.

REFERENCES

Backx, P., D. Yue, J. Lawrence, E. Marban, and G. Tomaselli. 1992. Molecular localization of an ion-binding site within the pore of mammalian sodium channels. *Science (Wash. DC)*. 257:248–251.

Becker, S., P. Prusak-Sochaczewski, G. Zamboni, A. G. Beck-Sickinger, R. D. Gordon, and R. J. French. 1992. Action of derivatives of μ-conotoxin GIIIA on sodium channels. Single amino acid substitutions in the toxin separately affect association and dissociation rates. *Biochemistry*. 31:8229–8238.

Cai, M., and P. C. Jordan. 1990. How does the vestibule surface charge affect ion conduction and toxin binding in a sodium channel? *Biophys. J.* 57: 883–891.

Catterall, W. A. 1992. Cellular and molecular biology of voltage-gated sodium channels. *Physiol. Rev.* 72:S15–S48.

Chou, P. Y., and G. D. Fasman. 1978. Empirical predictions of protein conformation. *Annu. Rev. Biochem.* 47:251–276.

Creighton, T. E. 1993. Proteins: Structure and Molecular Properties. 2nd ed. W. H. Freeman and Co., New York. 201–269.

Dani, J. A. 1986. Ion-channel entrances influence permeation: net charge, size, shape, and binding considerations. *Biophys. J.* 49:607–618.

Doyle, D., Y. Guo, S. L. Lustig, J. Satin, R. B. Rogart, and H. A. Fozzard. 1993. Divalent cation competition with [^{3}H]saxitoxin binding to tetrodotoxin-resistant and -sensitive sodium channels. *J. Gen. Physiol.* 101:153–182.

Fersht, A. R., J.-P. Shi, J. Knill-Jones, D. M. Lowe, A. J. Wilkinson, D. M. Blow, P. Brick, P. Carter, M. M. Y. Waye, and G. Winter. 1985. Hydrogen bonding and biological specificity analyzed by protein engineering. *Nature (Lond.)*. 314:235–238.

Green, W. N., L. B. Weiss, and O. S. Andersen. 1987. Batrachotoxin-modified sodium channels in planer bilayers. *J. Gen. Physiol.* 89: 873–903.

Guy, H. R., and F. Conti. 1990. Pursuing the structure and function of voltage-gated channels. *Trends Neurol. Sci.* 13:201–206.

Heinemann, S. H., H. Terlau, and K Imoto. 1992a. Molecular basis for pharmacological differences between brain and cardiac sodium channels. *Pflügers Arch.* 422:90–92.

Heinemann, S. H., H. Terlau, W. Stühmer, K. Imoto, and S. Numa. 1992b. Calcium channel characteristics conferred on the sodium channel by single mutations. *Nature (Lond.)*. 356:441–443.

Hille, B. 1968. Pharmacological modifications of the sodium channels of frog nerve. *J. Gen. Physiol.* 51:199–219.

Hille, B. 1971. The permeability of the sodium channel to organic cations in myelinated nerve. *J. Gen. Physiol.* 58:559–619.

Hille, B. 1975. The receptor for tetrodotoxin and saxitoxin: a structural hypothesis. *Biophys. J.* 15:615–619.

Hille, B. 1992. Ionic Channels of Excitable Membranes. 2nd ed. Sinauer Associates, Inc. Sunderland, MA. 59–62.

Kao, C. Y. 1982. Actions of norterodotoxin on frog muscle and squid axon. *Toxicon.* 20:1043–1050.

Kao, C. Y. 1986. Structure-activity relations of tetrodotoxin, saxitoxin and analogues. *Ann. N.Y. Acad. Sci.* 479:52–67.

Kao, C. Y., and S. E. Walker. 1982. Active groups of saxitoxin and tetrodotoxin as deduced from action of saxitoxin analogs on frog muscle and squid axon. *J. Physiol. (Lond.)*. 323:619–637.

Kao, C. Y., and T. Yasumoto. 1985. Actions of 4-epitetrodotoxin and anhydrotetrodotoxin. *Toxicon.* 23:725–729.

Kao, C. Y., P. N. Kao, M. R. James-Kracke, F. E. Koehn, C. F. Wichmann, and M. K. Schnoes. 1985. Actions of epimers of 12-(OH)-reduced saxitoxin and of 11-(OSO_3)-saxitoxin on squid axon. *Toxicon.* 23:647–655.

Koehn, F. E., V. E. Ghazarossian, E. J. Schantz, H. K. Schnoes, and F. M. Strong. 1981. Derivatives of saxitoxin. *Bioorg. Chem.* 10:412–428.

Kontis, K. J., and A. L. Goldin. 1993. Site-directed mutagenesis of the putative pore region of the rat IIA sodium channel. *Mol. Pharmacol.* 43:635–644.

Krimm, S., and J. Mark. 1968. Conformations of polypeptides with ionized side chains of equal length. *Proc. Natl. Acad. Sci. USA.* 60:1122–1129.

Mahar, J., G. L. Lucacs, Y. Li, S. Hall, and E. Moczydlowski. 1991. Pharmacological and biochemical properties of saxiphilin, a soluble saxitoxin-binding protein from the bullfrog. *Toxicon.* 29:53–71.

Narahashi, T., J. W. Moore, and R. N. Posten. 1967. Tetrodotoxin derivatives. Chemical structure and blockage of nerve membrane conductance. *Science (Wash. DC)*. 156:976–979.

Narahashi, T. 1974. Chemicals as tools in the study of excitable membranes. *Physiol. Rev.* 54:813–889.

Noda, M., S. Shimazu, T. Tanabe, T. Takai, T. Kayano, T. Ikeda, M. Takahashi, H. Nakayama, Y. Kanaoka, N. Minamino, et al. 1984. Primary structure of *Electrophorus electricus* sodium channel deduced from cDNA sequence. *Nature (Lond.)*. 312:121–127.

Noda, M., H. Suzuki, S. Numa, and W. Stühmer. 1989. A single point mutation confers tetrodotoxin and saxitoxin insensitivity on the sodium channel-II. *FEBS Lett.* 259:213–216.

Numa, S., and M. Noda. 1986. Molecular structure of sodium channels. *Ann. N.Y. Acad. Sci.* 479:338–355.

Pimentel, G. C., and A. L. McClellan. 1960. The Hydrogen Bond. Freeman Sc. Co., London. 265–285.

Proegman, J. H., G. Drent, K. H. Kalk, and W. G. T. Hol. 1978. Structure of bovine liver rhodanese. *J. Mol. Biol.* 123:557–594.

Satin, J., J. W. Kyle, M. Chen, P. Bell, L. L. Cribbs, H. A. Fozzard, and R. B. Rogart. 1992. A mutant of TTX-resistant cardiac sodium channels with TTX-sensitive properties. *Science (Wash. DC)*. 256:1202–1205.

Schild, L., and E. Moczydlowski. 1991. Competitive binding interaction between Zn^{2+} and saxitoxin in cardiac Na-channels. *Biophys. J.* 59: 523–537.

Schrager, P., and C. Profera. 1973. Inhibition of the receptor for tetrodotoxin in nerve membranes by various modifying carbonyl groups. *Biochim. Biophys. Acta.* 318:141–146.

Sibanda, B. L., T. L. Blundell, and J. M. Thornton. 1989. Conformations of β-hairpins in protein structures. *J. Mol. Biol.* 206:759–777.

Strichartz, G. 1984. Structural determinants of the affinity of saxitoxin for neuronal sodium channels. *J. Gen. Physiol.* 84:281–305.

Tang, S., G. Mikala, A. Bahinski, A. Yatani, G. Varadi, and A. Schwartz.

1993. Molecular localization of ion selectivity sites within the pore of a human L-type cardiac calcium channel. *J. Biol. Chem.* 268:13026–13029.

Terlau, H., S. H. Heinemann, W. Stühmer, M. Pusch, F. Conti, K. Imoto, and S. Numa. 1991. Mapping the site of block by tetrodotoxin and saxitoxin on sodium channel–II. *FEBS Lett.* 293:93–96.

Tomaselli, G. F., H. B. Nuss, J. H. Lawrence, P. H. Backx, and E. Marban. 1993. A cysteine substitution in the P-region of the skeletal muscle sodium channel alters sensitivity to tetrodotoxin and divalent cations. *Biophys. J.* 64:A88. (Abstr.)

Williams, R. W., A. Chang, D. Juretic, and S. Loughran. 1987. Secondary structural predictions and medium range interactions. *Biochim. Biophys. Acta.* 916:200–204.

Wilmot, C. M., and J. M. Thornton. 1988. Analysis of different types of β-turns in proteins. *J. Mol. Biol.* 203:221–232.

Yang, L., and C. Y. Kao. 1992. Actions of chiriquitoxin on frog skeletal muscle fibers and implications for the tetrodotoxin/saxitoxin receptor. *J. Gen. Physiol.* 100:609–622.

Yang, L., C. Y. Kao., and T. Yasumoto. 1992a. Actions of 6-epitetrodotoxin and 11-deoxytetrodotoxin on the frog skeletal muscle fiber. *Toxicon.* 30: 635–643.

Yang, L., C. Y. Kao, and Y. Oshima. 1992b. Actions of decarbamoyloxysaxitoxin and decarbamoylneosaxitoxin on the frog skeletal muscle fiber. *Toxicon.* 30:645–652.

Actions of Chiriquitoxin on Frog Skeletal Muscle Fibers and Implications for the Tetrodotoxin/Saxitoxin Receptor

L. YANG and C. Y. KAO

From the Department of Pharmacology, State University of New York Downstate Medical Center, Brooklyn, New York 11203

ABSTRACT Chiriquitoxin (CqTX) from the Costa Rican frog *Atelopus chiriquensis* differs from tetrodotoxin (TTX) only in that a glycine residue replaces a methylene hydrogen of the C-11 hydroxymethyl function. On the voltage-clamped frog skeletal muscle fiber, in addition to blocking the sodium channel and unrelated to such an action, CqTX also slows the activation of the fast potassium current in ~40% of the muscle fiber population. At pH 7.25, CqTX is as potent as TTX in blocking the sodium channel, with an ED_{50} of 3.8 nM. Its ED_{50}'s at pH 6.50 and 8.25 are 6.8 and 2.3 nM, contrasted with 3.8 and 4.3 nM for TTX. These differences are attributable to changes in the chemical states in the glycine residue. The equipotency of CqTX with TTX at pH 7.25 is explainable by an intramolecular salt bridge between the amino and carboxyl groups of the glycine function, all other surface groups in TTX and CqTX being the same. From available information on these groups and those in saxitoxin (STX), the TTX/STX binding site is deduced to be in a pocket 9.5 Å wide, 6 Å high, and 5 Å deep. The glycine residue of CqTX probably projects out of the entrance to this pocket. Such a view of the binding site could also account for the actions of STX analogues, including the C-11 sulfated gonyautoxins and the 21-sulfocarbamoyl analogues. In the gonyautoxins the sulfate groups are equivalently placed as the glycine in CqTX, whereas in the sulfocarbamoyl toxins the sulfate groups extend the carbamoyl side-chain, leading to steric hinderance to productive binding.

INTRODUCTION

Chiriquitoxin (CqTX) is an analogue of tetrodotoxin (TTX) found in the skin and eggs of *Atelopus chiriquensis*, a harlequin frog of the central highlands of Costa Rica (Kim, Brown, Mosher, and Fuhrman, 1975; Pavelka, Kim, and Mosher, 1977). In

Address reprint requests to Dr. C. Y. Kao, Department of Pharmacology (Box 29), SUNY Downstate Medical Center, 450 Clarkson Ave, Brooklyn, NY 11203.

Dr. Yang's permanent address is Department of Physiology, Kunming Medical College, Kunming, Yunan, China.

The views expressed in this paper are ours, and do not reflect those of our granting agencies.

J. GEN. PHYSIOL. © The Rockefeller University Press · 0022-1295/92/10/0609/14 $2.00
Volume 100 October 1992 609–622

those earlier studies, CqTX was known to retain the basic structure of TTX but to differ in the C-11 position by having a large substituent. In mouse lethality assays (Kim et al., 1975) and on the isolated frog skeletal muscle fiber it had the same specificity of action and potency as TTX (Kao, Yeoh, Goldfinger, Fuhrman, and Mosher, 1981). However, insufficient material was then available for a full clarification of the chemical structure or a definitive study of its actions on specific ionic channels. Repeated attempts to collect more material were unsuccessful until June 1988. Using current separation methods and a high pressure liquid chromatography TTX analyzer, CqTX was isolated and purified. Its structure has also been determined (Yotsu, Yasumoto, Kim, Naoki, and Kao, 1990).

We report here our studies of the actions of this new batch of CqTX on the functions of the sodium and potassium channels of the voltage-clamped, isolated frog skeletal muscle fibers. The significance of these studies extends beyond a mere comparison of CqTX with TTX. In recent years the structure–activity relations of some analogues of both TTX and saxitoxin (STX) have been clarified to a point where most active surface groups of these toxin molecules have been identified (for summary, see Kao, 1986; also Hu and Kao, 1991; Yang, Kao, and Yasumoto, 1992*a*; Yang, Kao, and Oshima, 1992*b*). Because the actions of CqTX are unique among TTX analogues, knowledge of its structure and actions permits us to draw some inferences on the probable physical dimensions of the TTX/STX binding site, and also to speculate on its possible location.

MATERIALS AND METHODS

CqTX was isolated from the skin of *A. chiriquensis* and its structure was determined by various spectroscopic methods, including mass spectrometry, ^{1}H- and ^{13}C-NMR spectrometry, and infrared spectrometry. Some details in stereochemical configurations were confirmed by derivatization experiments. The chemical studies can be found in Yotsu et al. (1990). The structure of CqTX is shown in Fig. 1. In comparison with that of TTX, the only difference is that a methylene hydrogen of the C-11 hydroxymethyl group of TTX is replaced by a glycine function in CqTX. Stated differently, CqTX has all the structural features of TTX, except that it has an additional –CH(NH_2)-COOH attached to the C-11 position.

The biological studies were performed on short segments of single isolated frog skeletal muscle fibers in a Vaseline gap voltage-clamp method (Hille and Campbell, 1976). Details of the procedures and methods of data acquisition and analysis can be found in other papers (Hu and Kao, 1991; Yang et al., 1992*a*). The actions of CqTX on both I_{Na} and I_K were studied.

Muscle fibers were held at −90 mV and depolarized by step increments until ~20 mV beyond the E_{Na}. To reduce errors attributable to series resistance, experiments were conducted in a bath solution containing only 44 mM Na^+. As a result, the E_{Na} was at +20 to +30 mV. The lower external Na^+ concentration does not alter the ED_{50} of the toxin (Hu and Kao, 1991). Current traces showing maximum I_{Na} and at E_{Na} were selected for detailed comparisons. The current at E_{Na} was I_K, and was used in previous studies of other analogues of TTX and STX primarily to assess the health of the fiber. However, CqTX also slows the activation of the fast I_K. Thus, the current records taken at E_{Na} were also useful for determining the rate of activation of I_K under various conditions. Time constants of the activation of the fast I_K were determined on the same fiber in the control and toxin-affected states (see Results). *t* tests for significance of differences of these data were based on pair comparisons.

The maximum I_{Na}'s in toxin-affected conditions were compared with those in control (no toxin) states, and the normalized relation (I'_{Na}/I_{Na}) was used for dose–response curves. The

small amount of I_K present at this voltage does not affect the ED_{50} determinations (Yang et al., 1992*a*). Least-squares linear regression lines were fitted to data in Hill plots of log $(1\text{-}P)/P$ ($P = I'_{Na}/I_{Na}$) vs. log toxin concentration. Standard errors of estimate were also obtained. ED_{50}'s and their standard errors were taken at $(1\text{-}P)/P = 1$ (Hu and Kao, 1991). *t* tests for significance of differences in the sodium channel blocking effect were based on unpaired group comparisons.

RESULTS

General Description

Although it is generally held that TTX affects only the sodium channel, recent studies on two analogues of TTX modified in the C-6 position indicate that there may be

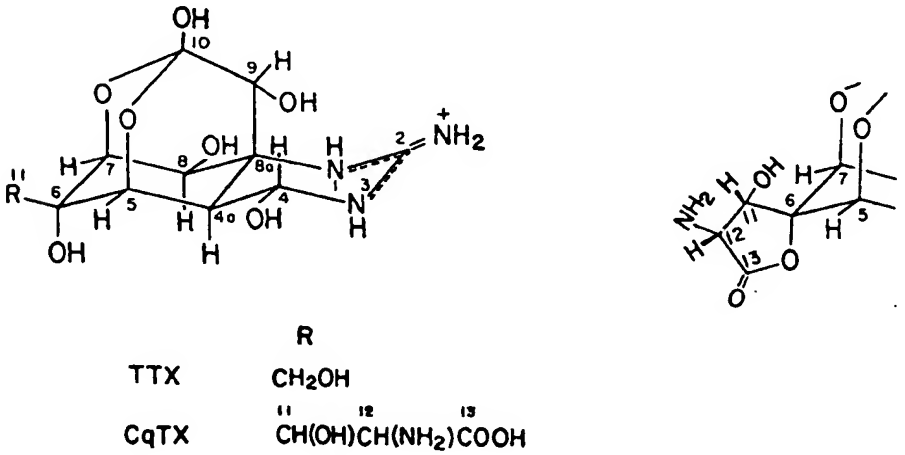

FIGURE 1. Chemical structure of CqTX compared with that of TTX. Note that CqTX contains all the features of TTX except that it has an additional glycine moiety on C-11. In TTX, and probably also in CqTX, the C-10 −OH group has a pKa of 8.8. In CqTX, the C-12 amino group has a pKa of ~9 and the C-13 carboxyl group has a pKa of ~2. These properties probably influence the sodium channel blocking action of CqTX at various pH's.

some exceptions (Yang et al., 1992*a*). In about half of the muscle fibers from *Rana temporaria*, TTX and 11-deoxyTTX, which retains the general configuration of the groups around C-6, significantly slow the activation of the fast I_K. 6-*epi*TTX, in which the -OH and the hydroxymethyl group of C-11 are in an epimeric configuration from that in TTX, does not cause significant slowing of the I_K. Fig. 1 shows that CqTX shares the general structural features of TTX at the C-6 position; Fig. 2 shows that in some fibers it also shares the effect of slowing the fast I_K. In such fibers, while I_{Na} is markedly reduced and eventually blocked, the fast I_K is also appreciably slowed. At 10 ms of a depolarizing step the I_K can be reduced by variable amounts, but at 20 ms it has usually reached the same amplitude as in the control state.

Effect of CqTX on Potassium Current

Because I_K is rather variable from fiber to fiber and even in the same fiber at different times, we used an arbitrary criterion to determine whether a toxin slowed the fast I_K. The time constants (τ) of the first 2 ms of the I_K of the pretoxin and recovered states were separately determined and then averaged. The averaged control τ was compared with that of the toxin-affected state. If the latter exceeded the former by 10%, we selected that fiber as having had its I_K slowed. Table I gives a summary of these comparisons. Of 36 fibers used for this study, 14 showed some slowing of the I_K. At 1

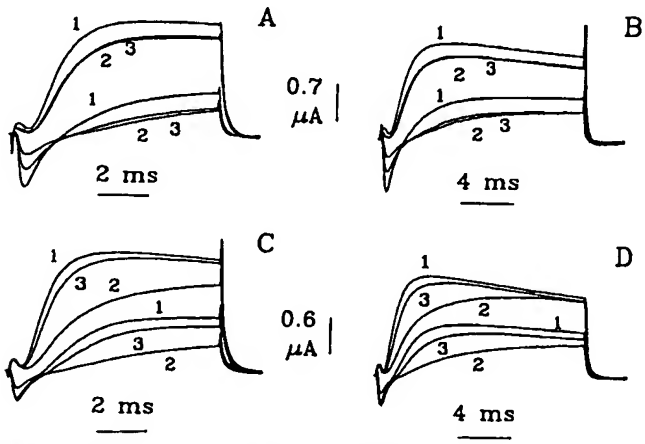

FIGURE 2. Effect of CqTX on I_{Na} and I_K of frog skeletal muscle fiber. Two different fibers (*A* and *B* from one; *C* and *D* from the other) in bath medium containing 44 mM Na^+. Holding potential −90 mV. Currents produced by two voltage steps are shown, one showing maximum inward I_{Na} and the other, at E_{Na}, showing I_K. In all panels, traces marked *1* denote the control state. In *A* and *B*, traces marked *2* denote responses to 4 nM CqTX, and traces marked *3* denote responses to 8 nM CqTX. In *C* and *D*, traces marked *2* denote responses to 2 nM CqTX, and traces marked *3* denote the recovered state. *A* and *C* are at fast sweep; total duration is 10 ms. *B* and *D* are at slower sweep; total duration is 20 ms. In addition to reducing I_{Na}, CqTX can also slow fast I_K without appreciably reducing total I_K. This feature is best shown in *C* and *D*, where the seemingly reduced I_K at 10 ms (*C*) is no different from the control state at 20 ms (*D*). The effect of CqTX is nearly fully reversible (*C* and *D*). In *A* and *B*, increasing concentrations of CqTX increased reduction of I_{Na}, but had no similar effect on the slowing of I_K. See text for additional reasons why the slowing of I_K is independent of block of I_{Na}.

nM CqTX generally did not cause any significant slowing of the I_K, even though it could reduce I_{Na} by ~20% (see Fig. 5). In 2–40-nM concentrations CqTX often caused some slowing, but the degree of slowing was not dependent on the concentration (Fig. 2, *A* and *B*). In those fibers in which slowing occurred, I_K usually recovered when CqTX was washed out. On subsequent application of another dose of CqTX, usually of a higher concentration, a lesser degree of slowing of I_K often occurred.

No influence of TTX. At pH 7.25, the ED_{50}'s of CqTX and TTX are the same, and like TTX, CqTX does not affect the onset or decay of the I_{Na} (see below). These

TABLE 1

Effect of CqTX on the Rate of Activation of the Fast Potassium Current

Concentration	Fibers	Time constant (τ) of fast I_K		*P*
		Control	Toxin	
nM		*ms*		
1	12	0.61 ± 0.02	0.62 ± 0.02	>0.05
2	10	0.61 ± 0.02	0.69 ± 0.04	<0.05
4	22	0.60 ± 0.01	0.67 ± 0.02	<0.05
8	8	0.63 ± 0.02	0.73 ± 0.02	<0.05
16	8	0.45 ± 0.02	0.56 ± 0.04	<0.05

All values are means ± SEM, with Fibers referring to the number of fibers used. Altogether 36 fibers were used, some of them for multiple doses of CqTX. Most fibers used for 16 nM came from frogs in May; fibers for all others came from frogs in July–September. *P* denotes *P* value in paired *t* test.

observations suggest that the affinity of the two toxins for the binding site are similar. The following experiments on the interaction between CqTX and TTX were conducted with concentrations of TTX 10–100-fold higher than that of CqTX to skew the mass-action equilibrium in favor of TTX. Even under these conditions, the effect of CqTX on I_K was not influenced by the presence of TTX, whether TTX was applied before or after CqTX.

Fig. 3 is an example of a high concentration of TTX that did not prevent CqTX from slowing the fast I_K. The I_{Na} was fully blocked by 40 nM of TTX, and the fast I_K

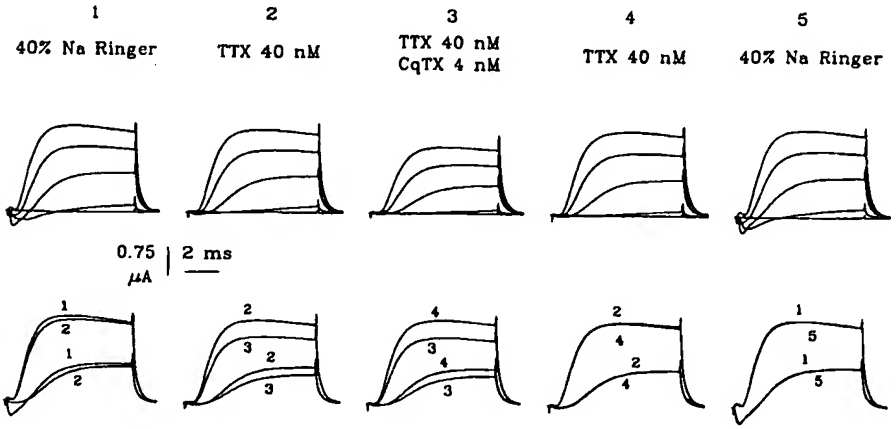

FIGURE 3. Prior action of TTX has no effect on the slowing of I_K by CqTX. (*Top row*) Current traces in various conditions sequentially as marked on top. Holding potential −90 mV; currents result from step voltages of −65, −40, −15, −10, and +35 mV. (*Bottom row*) Superimposed current tracings show different effects, with the number of the trace referring to the conditions marked above the top row. 40 nM TTX (panel *2*) fully blocked I_{Na} but only slightly and insignificantly affected fast I_K. An additional CqTX (panel *3*) markedly slowed fast I_K. This effect was reversible (panel *4*). When TTX was removed (panel *5*), both I_{Na} and I_K reversed fully.

was slightly slowed (panels *1* and *2*). When 4 nM of CqTX was applied, no additional effects on I_{Na} could be detected. The fast I_K was appreciably slowed, and the I_K at 10 ms was substantially lower than before (panels *2* and *3*). When CqTX was removed, the rate of activation of I_K recovered to that in TTX (panel *4*; compare with panel *2*). When TTX was also removed, both I_{Na} and I_K fully recovered (panel *5*; compare with panel *1*). This absence of influence of a prior application of TTX was demonstrated just as clearly in another fiber. Because the fibers were in very good condition, and the effects were clear, we did not repeat this sequence on more fibers.

High concentrations of TTX did not reverse the effect of CqTX on the I_K. In 10 fibers, I_{Na} was reduced by an ED_{50} dose (4 nM) of CqTX. In every fiber the fast I_K was appreciably slowed and the I_K at 10 ms was reduced. Then a high concentration of TTX (100 nM in four fibers and 400 nM in six fibers) was applied. While I_{Na} now became fully blocked, no further change in the I_K was seen. In every case the toxins were allowed to act for at least 8 min to reach steady state. Since the effect of TTX on I_K was usually less than that of CqTX, if the high concentration of TTX had reversed the effects of CqTX on I_K, one might have expected some recovery. Instead, the I_K at 10 ms in CqTX was 1.07 ± 0.11 μA (mean ± SEM of 10 fibers), compared with 0.99 ± 0.11 μA in a combination of CqTX and TTX.

No influence of $[Na^+]_o$ or of direction of I_{Na}. In addition to the apparently independent actions of TTX and CqTX on the I_K, other evidence shows that the effect of CqTX on the I_K is unrelated to functions of the sodium channel. In a Na^+-free bathing solution, CqTX caused as much slowing of the I_K as it did in 44 mM Na^+. Moreover, slowing of I_K was seen whether the I_{Na} was inward or outward.

The slowing of the fast I_K by CqTX is qualitatively similar to that seen with TTX and 11-deoxyTTX in about half of the muscle fiber population (Yang et al., 1992*a*). From all the above observations, we conclude that the slowing of the fast I_K is not related to the sodium channel blocking action of these toxin molecules, but that it is somehow related to the configurations of the C-6 groups common to all three. See Discussion for further comments.

Effect of CqTX on Sodium Current

Similar mechanism to that of TTX. Because CqTX slows the I_K in an appreciable fraction of the fiber population, a question arises as to whether it might have slowed the inactivation of I_{Na} such that some overlap of currents might be responsible for slowing the I_K. To examine this problem, experiments were performed on fibers in which the I_K had been blocked by applying Cs^+ to the end pools and allowing it to diffuse into the nodal area. Fig. 4 shows a typical example of such an experiment. In the control state, only the inward I_{Na} was seen. Upon action of 4 nM of CqTX the I_{Na} was reduced but there was no prolongation of the decay phase. When the toxin-affected I_{Na} is scaled to match the peak of the control I_{Na}, the currents are superimposed, with no detectable differences in either the onset or decay kinetics. The same results were seen in nine other fibers. Thus, the mechanism of action of CqTX on I_{Na} is apparently similar to that of TTX.

Dose–response relation. Fig. 5 shows the dose–response relation of CqTX on the I_{Na} at pH 7.25. As in the case of TTX, the data fit well a bimolecular reaction scheme where one toxin molecule interacted with one receptor site. This point is reinforced

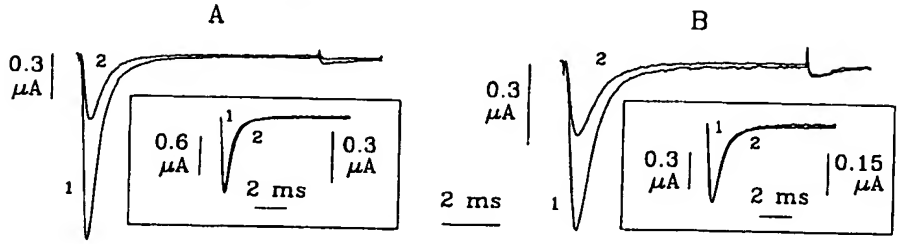

FIGURE 4. CqTX does not affect the rate of inactivation of I_{Na}. Two different fibers, both with I_K blocked by Cs^+. Holding potential −90 mV; step voltages to +10 mV. Traces marked *1* are maximum I_{Na} in control state; traces marked *2* are maximum I_{Na} in 4 nM CqTX (ED_{50}). (*Insets*) Traces *2* up-scaled to have peaks coincide with those of traces *1*, showing the absence of effect of CqTX on the kinetics of onset or decay of I_{Na}.

by the slope of 1.1 in the Hill plot where log $(1\text{-}P)/P$ ($P = I'_{Na}/I_{Na}$) is plotted against log toxin concentration. The ED_{50} of CqTX of 3.8 nM is not statistically significantly different from that of TTX, which is 4.1 nM (see Yang et al., 1992*a*).

Effect of pH on the dose–response relation. Because various toxin molecules contain ionizable groups, alterations in pH have been useful in correlating chemical changes with potency differences. Also, because the actions of CqTX are rather similar to those of TTX, it is instructive to examine the influence of pH on the actions of CqTX in comparison with those of TTX. In TTX, the C-10 −OH has a pKa of 8.8. It is more potent at pH 7.25 than at pH 8.25, with a relative potency that agrees well with the relative abundance of the protonated species of the C-10 hydroxyl group (Hu and Kao, 1991). Although there is no direct information on the property of the C-10

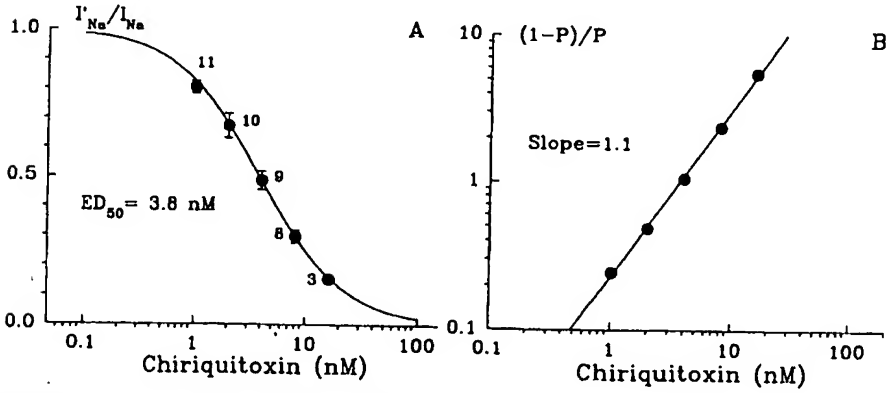

FIGURE 5. Dose–response relation of CqTX in blocking I_{Na} at pH 7.25. (*A*) Relative residual I_{Na} vs. log concentration of CqTX. The solid curve represents a bimolecular reaction scheme. The number attached to each point denotes the number of individual fibers from which data are obtained. Symbols denote mean values and vertical bars denote 1 SEM if larger than the symbol. The ED_{50} of 3.8 nM is not statistically different from that of 4.1 nM TTX (see text). (*B*) Hill plot, where $P = I'_{Na}/I_{Na}$. ED_{50} is determined when $(1\text{-}P)/P = 1$. A slope of 1.1 is consistent with a bimolecular reaction.

group in CqTX, because of similarities in chemical structures to TTX one might assume the pKa to be about the same as that of TTX. On this basis, one might expect CqTX to be similarly more potent at pH 7.25 than at 8.25.

Fig. 6 shows that, in actuality, CqTX is appreciably more potent at pH 8.25 (ED_{50}, 2.3 nM) than it is at pH 7.25 (ED_{50}, 3.8 nM; $P = 0.01$). Also, at pH 8.25 CqTX is significantly more potent than TTX (ED_{50}, 4.3 nM; $P < 0.001$, group comparison with data in Hu and Kao, 1991). These differences are probably not due to differences in protonation of the C-10 group, but are attributable to dissociable groups in the glycine function of CqTX.

At pH 6.50, increments in the protonated species of the C-10 group over that present at pH 7.25 are small, and the potency of TTX is slightly lower (ED_{50}, 3.8 nM), possibly because of a decrease in the density of surface negative charges (see discussion in Hu and Kao, 1991). For CqTX, however, the potency at pH 6.50 (ED_{50},

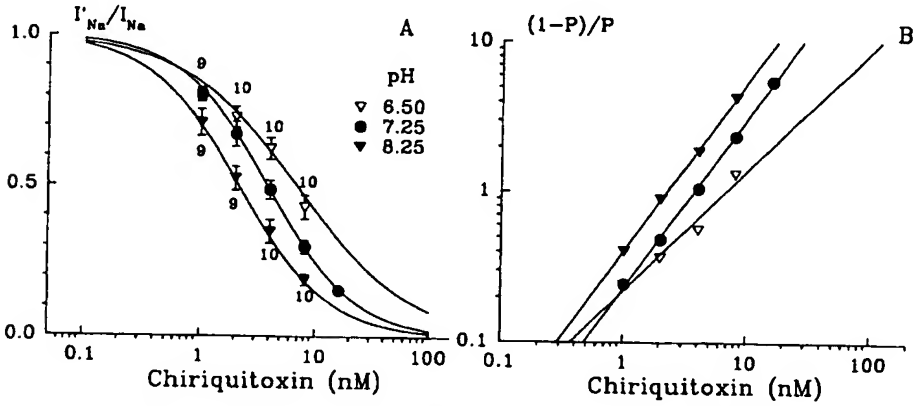

FIGURE 6. Influence of pH on the dose–response relation of CqTX in blocking I_{Na}. Conventions are similar to those in Fig. 5, from which data at pH 7.25 are taken. Slopes in the Hill plot are 0.9, 1.1, and 1.1, and ED_{50}'s are 6.8, 3.8, and 2.3 nM for pH 6.50, 7.25, and 8.25, respectively. See text for explanations of different potencies.

6.8 nM) is significantly less than that at pH 7.25 (ED_{50}, 3.8 nM; $P = 0.05$). Again, the reason for the difference must be sought in changes in the states of the glycine function.

DISCUSSION

Until the discovery of CqTX in 1975, no analogue or derivative of TTX was known to have anything but a small fraction of the potency of TTX. Thus, the chemical mechanism by which TTX blocked the sodium channel remained largely in the realm of speculation. CqTX was the first analogue of TTX to have substantial potency, and it rekindled studies of the structure–activity relations of the TTX family of molecules. Coincidentally, natural analogues of STX were also being discovered. The availability of analogues and derivatives of both TTX and STX fostered a re-examination of the

chemical mechanism of the sodium channel blockade. As shall become clear presently, because of its structure and its actions CqTX is of special importance in helping to consolidate a conception of the probable physical dimensions of the TTX/STX binding site.

Relation to Previous Work and Effect on I_K

The first study of the cellular actions of CqTX was made at a time when no voltage-clamp method capable of controlling the rapid sodium current was available for work on the frog skeletal muscle fiber (Kao and Yeoh, 1977). The maximum dV/dt of the action potential was used for an indirect assessment of sodium channel function, and constant current methods were used to study potassium channel function. In those experiments on muscle fibers of *Rana pipiens*, slowed repolarization of the action potential and a reduced level of delayed rectification were seen in some fibers at the same time that spike generation was impaired (Kao and Yeoh, 1977; Kao et al., 1981). Based on changes in the maximum dV/dt of the action potential, CqTX was judged to be as potent as TTX in blocking the sodium channel, but CqTX was also thought to have some effects on the potassium channel. The present results confirm that CqTX does have some effect on the potassium channel, but show that the effect is not a simple blockage as first believed. It is a more complex interference with the activation kinetics of the fast I_K and occurs in only about half of the population of muscle fibers. Because of variability, we do not have enough information at this time to fully explain that effect. All evidence in hand indicates that the effect on I_K is unrelated to the sodium channel blocking action. The effect on I_K is also seen with TTX and 11-deoxyTTX, but not with 6-*epi*TTX or neoSTX (Yang et al., 1992*a*). The common structural feature shared by CqTX, TTX, and 11-deoxyTTX is the configuration of the groups on C-6. Perhaps some potassium channel molecules, possessing some homology with the sodium channel (eg., Tempel, Papazian, Schwarz, Jan, and Jan, 1987) have a binding site for those groups.

Effect on I_{Na} and Influence of pH

In the sodium channel blocking effect, CqTX is unusual among TTX analogues in possessing a high degree of potency. With the exception of 11-oxoTTX (Wu, Yang, Kao, Yotsu, and Yasumoto, 1991), all other TTX analogues studied have varying degrees of reduced potency as compared with that of TTX, but CqTX is equally as potent as TTX. However, the pH influence on the potency of CqTX is rather different from that of TTX. Based on known chemical properties of CqTX (Fig. 1) we offer the following explanations for these differences:

In the glycine moiety of CqTX, the C-12 amino group has a pKa of ~9, and the terminal (C-13) carboxyl group has a pKa of ~2 (Yotsu et al., 1990). At pH 7.25 the C-12 amino group is mostly protonated, whereas the C-13 carboxyl group is deprotonated. An intramolecular salt bridge between those vicinal groups could largely remove them from any charge interactions with receptor groups in the sodium channel. As all the other groups in CqTX are the same as those in TTX, including the C-11 -OH group that forms a hydrogen bond with a receptor site (Yang et al., 1992*a*), the equipotency of CqTX and TTX is not difficult to understand,

provided a satisfactory explanation can be found for the absence of steric influences of the glycine moiety (see below).

Why is the pH influence on potency so different between TTX and CqTX? For TTX and STX between pH 6.50 and 8.25, differences in the chemical states of the toxin molecules are the most important factors in influencing potency (Hu and Kao, 1991). In TTX, changes in pH between 6.50 and 8.25 primarily affect the protonation of the C-10 -OH group, a condition that probably pertains to CqTX as well. In CqTX, however, the glycine function has two additional ionizable groups sensitive to pH changes. Under acidic conditions, the C-13 carboxyl group in CqTX tends to form an intramolecular lactone with the C-6 -OH (Yotsu et al., 1990; see also Fig. 1). Although pH 6.50 is less drastic than the conditions of those chemical studies, there may be a change in the equilibrium between CqTX and CqTX-lactone, shifting more toward the lactone form than it does at pH 7.25. In the lactone form, the C-6 -OH is lost and the C-11 −OH is fixed, probably in a different position from that in TTX. As both C-6 and C-11 −OHs participate in hydrogen bonds with site points in the receptor (Yang et al., 1992*a*), a shift in the equilibrium toward the lactone could account for the reduced potency of CqTX at pH 6.50.

At pH 8.25 TTX is less potent than at pH 7.25, but CqTX is appreciably more potent. Whereas the ED_{50}'s of TTX and CqTX at pH 7.25 are not significantly different, those at pH 8.25 are. These differences can be attributed to a decline in the protonated species of the C-12 amino group, a weakening of the intramolecular salt bridge with the terminal carboxyl, and an increasing role of the C-12 amino group in hydrogen bonding with receptor groups. However, it should be recognized that when the ED_{50} for reducing I_{Na} is taken as the K_d of the toxin receptor interaction, the difference in the ED_{50}'s at pH 7.25 and 8.25 reflects a difference in the Gibbs free energy of binding ($\Delta G = -RT \ln K_d$) of only ~1.5 kJ/mol.

Implications for the TTX/STX Receptor

In addition to electronic factors, steric factors also influence the docking orientation of a toxin molecule onto its receptor. In earlier work, three stereospecifically similar groups that participate in biological activity have been identified in the TTX and STX molecules (summarized in Kao, 1986): the 1,2,3 guanidinium of TTX and the 7,8,9 guanidinium of STX, the C-9 and C-10 hydroxyls of TTX, and the C-12 hydroxyls of STX. The N-1 hydroxyl of neoSTX was found to have an influence in binding to the receptor under some conditions (Hu and Kao, 1991). More recently, two analogues each of TTX (6-*epi*TTX and 11-deoxyTTX) and STX (deoxydecarbamoylSTX and decarbamoylneoSTX) have provided significant new information on the active groups in the TTX and STX molecules (Yang et al., 1992*a*, *b*). Briefly, the C-6 end of the TTX molecule was found to be active; also, when the active guanidinium groups and the pair of −OHs (see above) of the two toxin molecules were aligned, the carbonyl oxygen of STX corresponded to the C-6 −OH of TTX, while the amino group in the carbamoyl function of STX corresponded to the C-11 −OH of TTX. Since these active groups present themselves on all surfaces of the toxin molecules, we deduced that the TTX/STX binding site must be located in a crevice or a fold of the sodium channel protein.

Combining the present results with the earlier deduction, the TTX/STX binding

site can be viewed as being a pocket ~9.5 Å wide, 6 Å high, and 5 Å deep (Fig. 7; also Kao and Yang, 1992). In it are seven site points (designated sites *a–g*), which interact with various surface groups of either the TTX or the STX (and neoSTX) molecule. The CqTX molecule could have an additional reactive site point complementary to the C-12 $-NH_2$. However, the most impressive feature of CqTX is that in spite of the additional steric volume provided by the glycine function, it is very similar to TTX in potency. One possible explanation is that when bound productively to the receptor, the CqTX molecule is so oriented that the glycine function faces, and possibly protrudes out of, the entrance to the binding site, hence the minor contributions of the additional reactive groups on CqTX.

An attractive aspect of such a view of the binding site is that it can also explain two features regarding STX analogues that have not been satisfactorily accounted for before. Since TTX and STX bind to the same receptor, this ability to accommodate a group of chemically different compounds adds to the general plausibility of the proposed view. Among STX analogues there are two sulfur-containing subfamilies, the C-11 (numbering system for STX) gonyautoxins, which contain large sulfate substituents on the C-11 position, and the 21-sulfocarbomoyl toxins, which contain a sulfate end on the carbomoyl side-chain (for summary, see Oshima, Sugino, and Yasumoto, 1989). For gonyautoxins, the $-OSO_3$ substituents on C-11 add both large steric volumes and strongly negative charges rather close to the critical C-12 gem-diols, yet their potencies are only minimally reduced (Kao, Kao, James-Kracke, Koehn, Wichmann, and Schnoes, 1985). On the other hand, the bulk and charges of the $-OSO_3$ groups in the sulfocarbomyl toxins at the end of a side-chain profoundly lower the potency. Both of these features can be explained by the proposed view of the TTX/STX receptor as situated in a pocket.

Molecular modeling shows that when the active guanidinium groups of TTX and STX are aligned, as are the C-9 and C-10 −OHs of TTX with the C-12 −OHs of STX, the C-11 sulfate groups of the gonyautoxins are stereochemically placed much like the glycine moiety of CqTX (Fig. 7). Perhaps their minimal influence on potency is also to be attributed to their projecting out of the entrance to the binding site pocket and being removed from nearby reactive site points. On the other hand, the sulfate groups on the 21-sulfocarbamoyl toxins extend the carbamoyl side-chain so much that steric hinderance interferes with the entry of the toxin into the binding site pocket. Understandably, when those sulfate groups are cleaved through acid hydrolysis (Shimizu, Kobayashi, Genenah, and Oshima, 1984), the product toxins become considerably more active because they are now freed of the steric interference and can productively occupy the binding site to block the sodium channel.

Observations on mutated sodium channels of rat brain suggest that negatively charged amino acid residues in short segments 2 between S5 and S6, at positions 384 and 387 of repeat I, and equivalently placed residues in repeats II, III, and IV strongly influence the actions of TTX and STX (Noda, Suzuki, Numa, and Stühmer, 1989; Kontis and Goldin, 1991; Terlau, Heinemann, Stühmer, Pusch, Conti, Imoto, and Numa, 1991). Mutating the anionic glutamate or aspartate to the uncharged glutamine or asparagine raises the ED_{50} for blocking I_{Na} by more than three orders of magnitude. We speculated that if glutamate 387 corresponded to our binding site *a*, then the carbonyl oxygen of asparagine 388 could represent our binding sites *b* and *c*

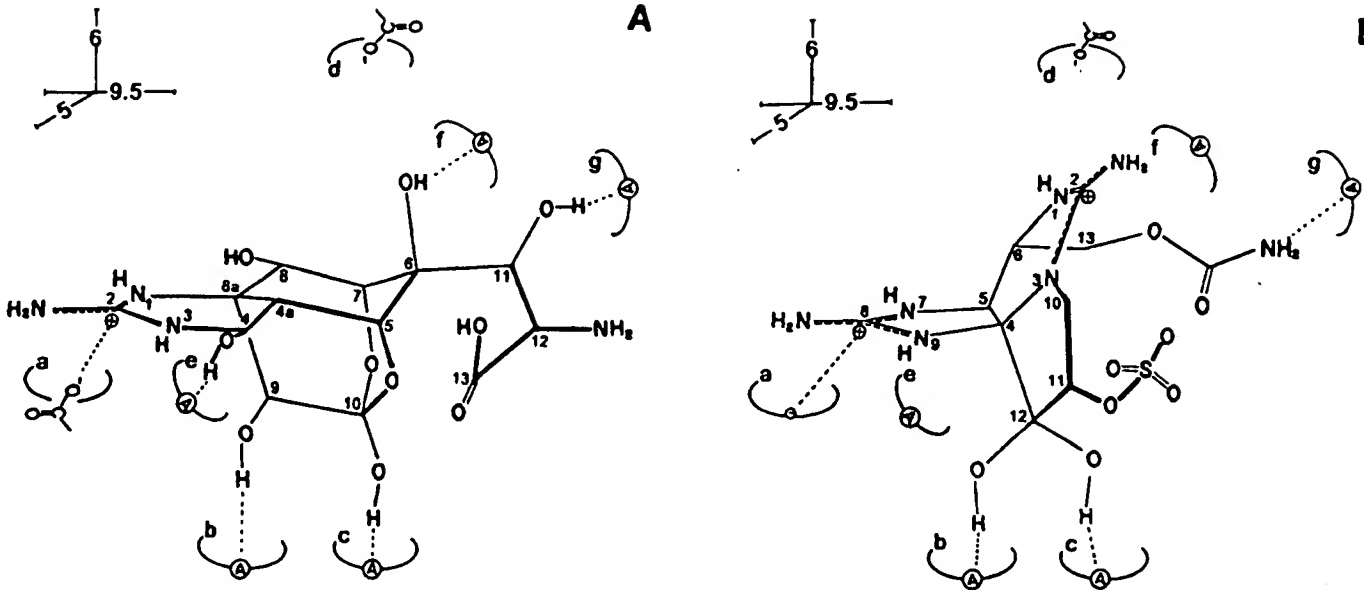

FIGURE 7. Possible dimensions and anchoring site points in the TTX/STX binding site. The binding site is in a pocket, being viewed head-on through the entrance of the pocket. Identified anchoring points in the binding site (sites *a–g*) have been shown to be complementary to specific groups in TTX, STX, and neoSTX molecules (see references in text). TTX and STX share site points *a*, *b*, *c*, *f*, and *g*; neoSTX has an additional site point *d*. Site point *e* is complementary to the C-4 −OH of TTX. (*A*) A molecule of CqTX is shown in perspective view in presumed correct docking orientation, with the glycine moiety protruding out toward the entrance. In spite of the large steric volume and additional charges in glycine, CqTX shares all the structural features of TTX and hence all the complementary site points. Its equipotency with TTX is due to glycine projecting out of the pocket of reactive sites. (*B*) A molecule of a gonyautoxin, sulfated on the C-11 of STX, is shown in perspective view, occupying the same binding sites. The sulfate group also projects out of the pocket, accounting for the relatively minor effect it has on the potency of STX. In 21-sulfocarbamoylSTX (not shown), the sulfate group on the end of the carbamoyl side-chain would cause steric hinderance for the toxin molecule to occupy the binding site; hence its weakness. When such end sulfate groups are hydrolyzed off in acid conditions, the steric hinderance is removed and toxin potency increases, sometimes many times.

(Yang et al., 1992*a*, *b*). However, the situation is complicated by the contradictory observations that mutants containing arginine 388 showed no significant difference in sensitivity to TTX and STX (Terlau et al., 1991), whereas in the sodium channel of rat cardiac myocyte TTX/STX insensitivity is associated with the presence of arginine at 388 (Rogart, Cribbs, Muglia, Kephart, and Kaiser, 1989). Not unexpectedly, molecular models of short segments of amino acid residues from 383 to 390 do not show any folds that could envelop the TTX or the STX molecule. However, in the concentric model proposed by Guy and Conti (1991), the TTX/STX binding site could straddle two repeats, which could contain the appropriate residues to provide the crevice that serves as the toxin binding site. Experimental identification of the binding site would require specific marker compounds that need to be made. However, a successful identification of the binding site could add much to a better understanding of the structure and function of the sodium channel.

We thank Drs. B. Q. Wu and M. Yotsu (Tohoku University, Sendai, Japan) for helpful suggestions and comments on our interpretations, as well as Prof. Olaf Andersen (Cornell University Medical College, New York) for comments on a draft of the manuscript.

This work is supported by a grant from the National Institute of Neurological Disorders and Stroke (NS-14551) and a contract from the U. S. Army Medical Research and Development Command (DAMD17-87-C-7094).

Original version received 21 November 1991 and accepted version received 18 May 1992.

REFERENCES

Guy, H. R., and F. Conti. 1990. Pursuing the structure and function of voltage gated channels. *Trends in Neurosciences.* 16:201–206.

Hille, B., and D. T. Campbell. 1976. An improved vaseline-gap voltage clamp for skeletal muscle fiber. *Journal of General Physiology.* 67:265–293.

Hu, S. L., and C. Y. Kao. 1991. Interactions of neosaxitoxin with the sodium channel of the frog skeletal muscle fiber. *Journal of General Physiology.* 97:561–578.

Kao, C. Y. 1986. Structure-activity relations of tetrodotoxin, saxitoxin, and analogues. *Annals of the New York Academy of Sciences.* 479:52–67.

Kao, C. Y., P. N. Kao, M. R. James-Kracke, F. E. Koehn, C. F. Wichmann, and H. K. Schnoes. 1985. Actions of epimers of 12-(OH)-reduced saxitoxins and of 11-(OSO_3)-saxitoxin on squid axon. *Toxicon.* 23:647–655.

Kao, C. Y., and L. Yang. 1992. The tetrodotoxin/saxitoxin binding site. *Biophysical Journal.* 61:A110. (Abstr.)

Kao, C. Y., and P. N. Yeoh. 1977. Interactions of chiriquitoxin and tetrodotoxin with frog muscle fiber membrane. *Journal of Physiology.* 272:54P–55P.

Kao, C. Y., P. N. Yeoh, M. D. Goldfinger, F. A. Fuhrman, and H. S. Mosher. 1981. Chiriquitoxin, a new tool for mapping ionic channels. *Journal of Pharmacology and Experimental Therapeutics.* 217:416–429.

Kim, Y. H., G. H. Brown, H. S. Mosher, and F. A. Fuhrman. 1975. Tetrodotoxin: occurrence in *Atelopid* frogs of Costa Rica. *Science.* 189:151–152.

Kontis, K. J., and A. L. Goldin. 1991. Sodium channel structure/function: effects of negative charge mutations on block by TTX. *Society for Neuroscience Abstracts.* 17:954A. (Abstr.)

Noda, M., H. Suzuki, S. Numa, and W. Stühmer. 1989. A single-point mutation confers tetrodotoxin and saxitoxin insensitivity on the sodium channel II. *FEBS Letters.* 259:213–216.

Oshima, Y., K. Sugino, and T. Yasumoto. 1989. Latest advances in HPLC analysis of paralytic shellfish toxins. *In* Mycotoxins and Phycotoxins. S. Natori, K. Hashimoto, and Y. Ueno, editors. Elsevier Science Publishers B. V., Amsterdam. 319–326.

Pavelka, L. A., Y. H. Kim, and H. S. Mosher. 1977. Tetrodotoxin and tetrodotoxin-like compounds from the eggs of the Costa Rica frog *Atelopus chiriquensis*. *Toxicon*. 15:135–139.

Rogart, R. B., L. L. Cribbs, L. K. Muglia, D. D. Kephart, and M. W. Kaiser. 1989. Molecular cloning of a putative tetrodotoxin-resistant rat heart Na^+ channel isoform. *Proceedings of the National Academy of Sciences, USA*. 86:8170–8174.

Shimizu, Y., M. Kobayashi, A. Genenah, and Y. Oshima. 1984. Isolation of side-chain sulfated saxitoxin analogs. *Tetrahedron*. 40:539–544.

Temple, B. L., D. M. Papazian, T. L. Schwarz, Y. N. Jan, and L. Y. Jan. 1987. Sequence of a probable potassium channel component encoded at Shaker locus of Drosophila. *Science*. 237:770–775.

Terlau, H., S. H. Heinemann, W. Stühmer, M. Pusch, F. Conti, K. Imoto, and S. Numa. 1991. Mapping the site of block by tetrodotoxin and saxitoxin of sodium channel II. *FEBS Letters*. 293:93–96.

Wu, B. Q., L. Yang, C. Y. Kao, M. Yotsu, and T. Yasumoto. 1991. 11-Oxotetrodotoxin, a potent analogue of tetrodotoxin. *Biophysical Journal*. 59:261*a*. (Abstr.)

Yang, L., C. Y. Kao, and T. Yasumoto. 1992*a*. Actions of 6-*epi* tetrodotoxin and 11-deoxytetrodotoxin on the frog skeletal muscle fiber. *Toxicon*. 30:635–643.

Yang, L., C. Y. Kao, and Y. Oshima. 1992*b*. Actions of deoxydecarbamoylsaxitoxin and decarbamoylneosaxitoxin on the frog skeletal muscle fiber. *Toxicon*. 30:645–652.

Yotsu, M., T. Yasumoto, Y. H. Kim, H. Naoki, and C. Y. Kao. 1990. The structure of chiriquitoxin from the Costa Rican frog *Atelopus chiriquensis*. *Tetrahedron Letters*. 31:3187–3190.

To: Clint IWT Total 10 pages.
From: Leo MLP 2003. 11. 11

The Guanidinium Toxin Binding Site on the Sodium Channel

Harry A. FOZZARD, MD,
and Gregory LIPKIND, PhD

SUMMARY

Study of TTX and STX toxins and their interaction with cloned Na channels has led to a molecular model of the toxins' binding site. This model is able to explain isoform differences in binding affinity, allowing prediction of the structures of toxin-resistant channels. It provides an example of a detailed drug binding site that could serve as an example for drug engineering to improve affinity and specificity. The model has also suggested important molecular characteristics of the channel's permeation path, providing a wealth of ideas for study of this fundamental biophysical process at the molecular level. The model of the TTX and STX binding site outlines an approach to resolution of molecular structure and of certain structure-function relationships, and experimentation provoked by the model will assist in improving it. (Jpn Heart J 1996; 37: 683-692)

Key words: Guanidinium toxin Tetrodotoxin Saxitoxin Sodium channel Molecular modelling Vestibule Structure-function

THE guanidinium toxins, tetrodotoxin (TTX) and saxitoxin (STX), are highly poisonous marine toxins that have become extraordinarily valuable tools in the study of excitable tissues. They bind uniquely and with high affinity to voltage-gated sodium channels and block them completely. The usual vector for poisoning for TTX is the *fugu* (puffer fish), and for STX it is mussels, with ingestion of either toxin producing paralysis of respiration. However, the *fugu* does not synthesize TTX, but instead concentrates it via bacteria in its food chain. Similarly, STX is synthesized by dinoflagellates that are ingested by the shellfish. Other animals can also concentrate the toxins, presumably derived from their food.

Biophysical evidence points to a stoichiometric binding of the toxins to a shared site in the outer mouth or vestibule of the sodium channel pore and partly within the membrane field. Mutational studies with cloned mammalian sodium

From the Departments of Pharmacological & Physiological Sciences, Medicine, and Biochemistry and Molecular Biology, and the Committee on Cell Physiology, The University of Chicago, Chicago, USA.
Address for correspondence: Harry A. Fozzard, MD, Department of Pharmacological & Physiological Sciences, The University of Chicago, Chicago, IL 60637, USA.

channels has identified an involved stretch of amino acids in each of the four protein domains of the α-subunit. It has been possible to develop a molecular model of this binding site, which appears to include the channel's selectivity filter region, resulting in predictions about the molecular energetics of ion permeation and selectivity.

The Guanidinium Toxins

TTX and STX are small rigid cyclic molecules (TTX = 319 MW; STX = 299 MW). They have been synthesized and structurally determined by X-ray crystallography. TTX has an essential guanidinium group and carries one positive charge at physiological pH, and STX has two guanidinium groups with two positive charges. A number of naturally occurring analogs have been found, and others have been made synthetically, facilitating identification of critical active groups involved in toxin binding.[1,2] For TTX the most critical groups are the 1,2,3 guanidinium and the C9 and C10 hydroxyls, and for STX they are the 7,8,9 guanidinium and the two C12 hydroxyls. Presumably the 1,2,3 guanidinium is also important, but the analog evidence is less clear.

Narahashi and colleagues[3] demonstrated that TTX selectively blocks sodium current in excitable cells. It appears to block by occluding the external mouth of the channel pore,[4] by partial entry into the pore. There it coordinates noncovalently to a titrable carboxyl oxygen with a pK_a of 5–6[4,5] which is probably part of the channel's selectivity filter. The selectivity filter is about 20–30% into the membrane electric field, and this causes TTX binding to be somewhat voltage dependent.[6] STX competes with TTX, so the two toxins are likely to have overlapping binding sites.[7] Their binding is quite sensitive to monovalent and divalent ions in the outside solution, and the interaction appears to be competitive[5]. The toxins have minimal effects on the channel gating process, as judged by gating current measurements, consistent with the idea that they act as a plug. However, their block is use-dependent,[8-10] as if their binding sites are changed somewhat by the conformational alterations associated with gating of the channel.

Typical nerve and skeletal muscle Na channels are blocked by TTX with 1:1 stoichiometry with K_d of about 10 nM. However, cardiac Na channels are much less sensitive, with K_d of a few μM. STX also has a higher affinity for the nerve and skeletal muscle Na channels than for heart (Figure 1). This tissue difference in TTX/STX affinity was the first clue that the cardiac Na channel might be a different isoform. Kinetic studies have shown that both the association rates and the dissociation rates are different between the channel types.[11] The low affinity of the cardiac channels is not unique. For example, Na channels in

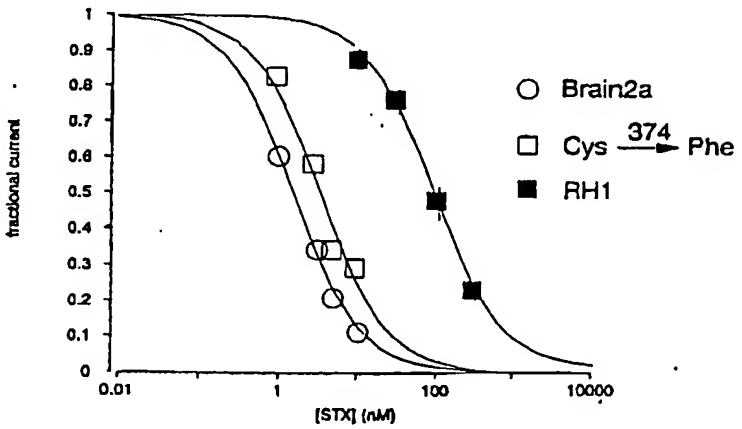

Figure 1. STX dose-response curves for block of the cardiac (RH1) and the nerve (Brain2a) Na channel α-subunits expressed in *Xenopus* oocytes. The STX dose-response curve for block of the cardiac isoform with Cys374 (cardiac isoform numbering) mutated to a Phe is also shown. The currents were generated by trains of voltage steps using the two-pipette voltage clamp method and the steady-state peak Na current is reported as a fraction of the current in the absence of drug.

the dorsal root ganglion belong to several populations, some with typical high TTX/STX affinity, some with low affinity, and some that are totally resistant.[12]

Sodium Channel Structure

Na channels are scarce membrane proteins that are difficult to purify, so TTX and STX were very important markers for the Na channel during the long process of purification and amino acid analysis that was necessary to prepare for cloning of the protein. The first Na channel to be cloned was from the eel electroplax, and the α-subunit is a 2000 amino-acid protein.[13] Subsequently, three Na channel α-subunits have been cloned from brain, two from skeletal muscle, and one from heart, all having 70–90% homology.[14] The embryonic isoform in skeletal muscle, also manifested after denervation of adult muscle, appears to be identical to the cardiac isoform. These mammalian isoforms of the α-subunits have been successfully expressed in heterologous cells. The cardiac isoform has been shown to have the permeation, gating, and pharmacological properties of native cardiac Na channels.[15] A number of non-mammalian Na channel isoforms have been cloned, and other mammalian nerve and muscle isoforms have now been found.[14] Brain Na channels have two small β subunits, and skeletal muscle has one.[16] The presence or role of β subunits for the cardiac channel or the others has not yet been resolved. All isoforms of the α-subunits show a similar topology, determined by hydropathy analysis and the sidedness of

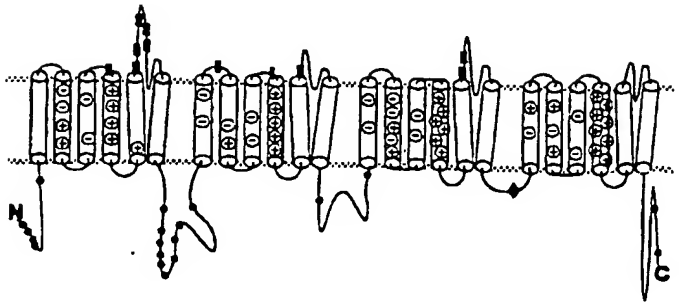

Figure 2. Likely topology of the cardiac Na channel α subunit. Number of charges in the putative membrane spanning regions are denoted. PKC site is denoted by ◆. Putative PKA sites (●) were taken as R/K X S/T or R X X S/T or R X S/T where X denotes any amino acid. Putative N-linked glycosylation sites (■) were defined by N X S/T where X is any amino acid except proline. (From,[28] with permission of the American Physiological Society)

certain antibody, glycosylation, and phosphorylation sites (Figure 2). There are 24 transmembrane segments, organized into four homologous sets of six segments that appear to form domains. The fourth transmembrane segment of each domain has negatively charged amino acids in every third position, which led Numa and colleagues[13] to suggest that these segments are the channel's voltage sensor.

The presence of four domains also led to the idea that the transmembrane path for ion transport was formed as a central pore that was surrounded by the four domains. Intuitive modeling of the molecule by Guy and colleagues[17] suggested that the pore was partially lined by an infolding of the extracellular segment between S5 and S6 of each domain that they called SS1 and SS2. In a brilliant set of mutational studies, Stühmer and colleagues[19] proved that these segments were indeed part of the permeation path, and were also part of the binding site for TTX and STX. Two carboxyls in each of domains I and II, a carboxyl in domain IV, and a lysine in domain III were all critical for binding of TTX and STX, confirming Hille's proposal that the toxins bound to carboxyl oxygens in the pore mouth. Further, their mutation to neutral amino acids reduced substantially the single channel conductance, as expected if the toxin site is in the permeation path.

Isoform Differences In Guanidinium Toxin Binding

Localization of the pore and toxin binding site, however, failed to explain the low cardiac affinity for the guanidinium toxins in comparison with brain and skeletal Na channels. All of the residues identified as critical for toxin binding by the experiments of Terlau et al[18] are identical in the cardiac isoform. Only two

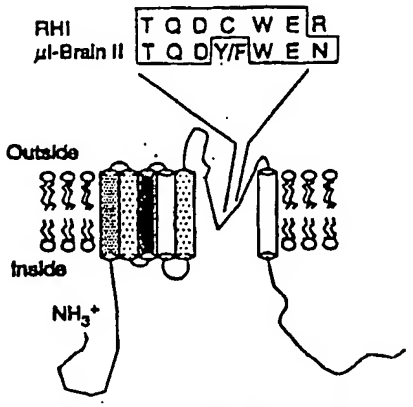

Figure 3. Depiction of the first domain of the Na channel α-subunit. The seven amino acid SS2 sequence is shown and the differences between the cardiac isoform (RHI) and the brain and skeletal muscle isoforms (μ1-BrainII) isoforms are indicated. Abbreviations for the amino acid residues are: C, Cys; D, Asp; E, Glu; F, Phe; N, Asn; Q, Gln; R, Arg; T, Thr; W, Trp; and Y, Tyr. (From,[10] with permission of the American Association for the Advancement of Science.)

residues differ between the isoforms in the four SS1–SS2 segments, a cysteine in place of a phenylalanine and an arginine in place of an asparagine (Figure 3). The cardiac channel also differs functionally in being especially sensitive to block by Cd^{2+}, and Cd^{2+} competes with STX binding.[5] Because cysteine is a logical amino acid for Cd^{2+} binding, Schild and Moczydlowski[19] further suggested that this is the residue responsible for the difference in toxin binding. Within a short time, overwhelming evidence was found to prove that the residue in that location was critical: Satin et al[10] replaced Cys in the cardiac isoform with Tyr or Phe and found an increase in toxin sensitivity to the levels seen in brain, Backx et al[20] replaced the Tyr in the skeletal muscle isoform with Cys and reduced toxin sensitivity dramatically, and Heinemann et al[21] replaced the Phe in the brain II isoform with Cys and reduced toxin sensitivity to the levels seen in heart. Change of the Arg/Asn residue had only small effects on the toxin block, indicating that it had a minor role in the isoform difference.

A Model of the Guanidinium Toxin Site

At this point in our study of the toxin site the following information was available:

1. Crystallographically determined structures of the rigid TTX and STX molecules.
2. Knowledge of the toxin reactive sites from studies with toxin analogs.
3. Identification of 6–8 residues in the channel pore of brain, skeletal and

cardiac isoforms that are required for toxin binding.

4. Awareness of the specific residue responsible for isoform differences in binding.

It was reasonable to ask if we could use this information set to infer the structure of the toxin binding site, using the toxins as structural templates of the sites. Presumably the toxins correspond to a key that fits securely into their locks by close association with channel residues, in order to achieve their high affinity and selectivity. If this effort to visualize the toxin binding site was successful, then it is possible that removal of the toxin from the site would reveal the general structure of the mouth of the channel pore.

Our first task was to identify a possible secondary structure of the SS1–SS2 regions such that the critical residues for toxin interaction in the four domains that have been identified by mutational studies could face a potential binding pocket. The motif for binding in domain I involved two adjacent residues-Asp and Cys/Tyr/Phe- and after an intervening Trp another critical residue-Glu. This arrangement was unsuitable for α-helical or β-structures, but could occur in a reverse turn. We examined the probability of a β-turn in the SS1–SS2 segments

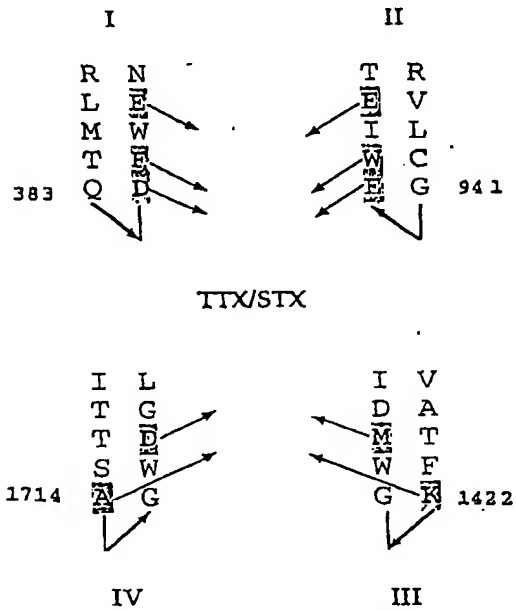

Figure 4. Structural motif for the TTX/STX binding site of the Na channel - an antiparallel arrangement of β-hairpins of domains I-IV. Residues that interact with the toxins are marked by the arrows. The residue numbers are according to the Brain2 isoform, and are for the ones located in positions $i + 1$ of β-turns. Relative orientation of β-turns of the four hairpins is shown by flat arrows connecting the beta1 and beta2 strands, and it corresponds to an overhead view. (From[42] with permission of the Biophysical Society).

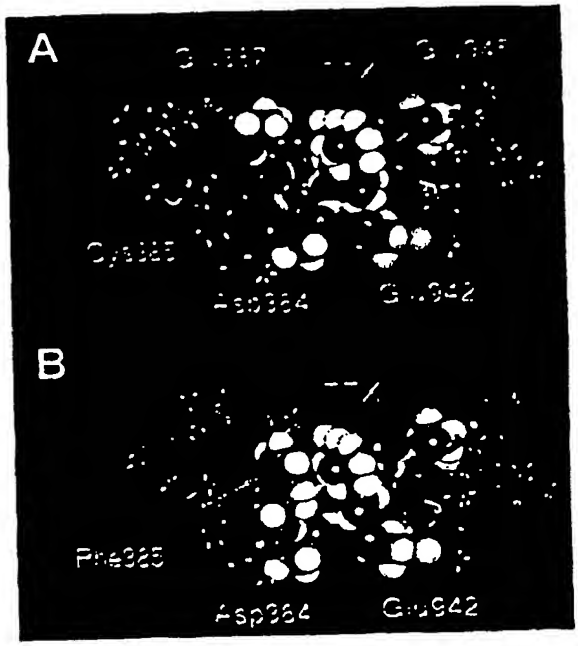

Figure 5. The Lipkind-Fozzard tetrodotoxin binding site model. TTX interacts with four residues on the β-hairpin model (green ribbon) of the domains I and II P segments. Asp384 and Glu387 are shown as space-filling residues from domain I β-hairpin and Glu942 and Glu945 are shown from domain II β-hairpin. In the model the guanidinium toxin interacts with Glu387, Asp384, and Glu942. The hydroxyls of the toxin interact with Glu945. (A) The cardiac structure for domain I, with a Cys in position 385. (B) Substitution of Phe in position 385, with the space-filling aromatic ring interacting with the toxin hydrophobic surface. The image is rotated slightly from that in panel A, to more clearly show the relationship. (From,[7] with permission of the American Physiological Society).

and found a site that fit the Chou-Fasman rules for such a turn in each of the SS1–SS2 segments. Using software for molecular modeling, we constructed from each segment β-hairpins that were energetically stable[22] (Figure 4). After constructing the toxin structures in the computer, we could dock TTX onto the domain I β-hairpin into an energetically satisfactory position and then dock the domain II β-hairpin onto the complex. The resulting binding pattern (Figure 5) was a set of three salt bridges between the two carboxyls of domain I and the inner one of domain II to the guanidinium group of TTX. The two hydroxyl groups on C9 and C10 interacted by hydrogen bonds with the outer carboxyl of domain II. Each channel residue-toxin interaction was about – 10 kcal/mol under the conditions of the model construction. Superimposing the 7,8,9 guanidinium of STX on the 1,2,3 guanidinium of TTX positioned the C12

hydroxyls of STX nearly exactly where the C9 and C10 hydroxyls of TTX were found. We therefore found that the same spatial arrangement of the domains I and II hairpins fit the STX molecule, but STX has a second guanidinium. This allowed docking of the domain IV hairpin onto the STX complex in a similar pattern, so that the domain IV carboxyl interacted with the second guanidinium of STX. The domain III hairpin was positioned symmetrically to allow modest non-bonding interactions, forming a four-hairpin structure. This model fits the data of Terlau et al[18] for the toxin binding site.

If this four-hairpin model has any resemblance to the TTX/STX binding pocket, then the isoform differences seen as a consequence of the Cys/Tyr/Phe residues should be predicted by the model. Replacement of Cys with Tyr or Phe in the model positioned the aromatic ring to have a hydrophobic interaction with the toxin (Figure 5). The change in binding energy estimated by the modeling program was about − 5 kcal/mol, similar to the − 4 kcal/mol estimated experimentally by Satin et al.[10]

Implications For Structure of the Channel Vestibule and Selectivity Filter

Removal of the toxin from the binding site model revealed a 12Å-deep funnel-like structure about 12Å on as side at the wide mouth, and narrowing to a 3 × 5Å opening at the narrow mouth. This narrow opening corresponded to the size predicted by Hille[23] for the Na channel selectivity filter from the sizes of permeating organic cations. The opening was surrounded by four aligned residues, one from each hairpin-Asp, Glu, Lys, and Ala. Heinemann et al[24] noticed the remarkable similarity of the SS1-SS2 regions of the Na and Ca channels, and similar alignment these four regions showed that the putative selectivity ring of the Na channel corresponded to four carboxyls in the Ca channel. They therefore substituted carboxyls in these positions in domains III and IV of the brain II Na channel in place of the naturally occurring Lys and Ala, and found that they had created a mutant channel that was permeable to Ca^{2+}. In their experiments the Lys to Glu mutation in domain III was the most effective. This dramatic demonstration of change in selectivity supported the idea that this ring of four amino acids in the Na channel constitutes part of its selectivity filter.

We explored the idea further by allowing a model of the Na^+ ion hydrated with six water molecules to interact with the putative selectivity ring in our model. It readily interacted with the two inner carboxyls of domains I and II with an energy of about 100 kcal/mol-equivalent to the hydration energy of Na^+. This interaction effectively dehydrated the ion, a step usually considered to be necessary for permeation. Ca^{2+} interacted with the two carboxyls, but with insufficient

energy to dehydrate the ion. However, if the Lys of domain II was replaced with a carboxyl, the three carboxyls were positioned correctly to dehydrate Ca^{2+}, as needed for its permeation, agreeing with the experiments of Heinemann et al.[24] K^+ ions interacted with the domain I and II carboxyls with the same energy as for Na^+, so this analysis did not explain the 10:1 selectivity of the channel for Na^+ over K^+. The model exhibits several characteristics necessary for the Na channel selectivity filter, but the model calculations cannot provide proof of its accuracy. More likely, the entire vestibule participates in the energetic steps that allow permeation.

Several approaches to test and refine the Na channel vestibule-selectivity filter model are being pursued. First, other ligands that bind to the pore can be studied in mutated channels, including TTX/STX analogs and the μ-conotoxin peptides derived from snails. Second, location of component amino acid side chains can be explored by substitution with cysteines, with which divalent ions and organic sulfhydryl reagents may interact. Third, the nature and location of other residues involved in the permeation and/or selectivity process can be found by detailed biophysical analysis of point mutations substituting residues of different size, hydrophobicity, and charge. Several of these efforts are now in progress.[25-27] Similar efforts to model the K channel pore from toxin interaction and mutation of critical residues might be revealing,[28] because that channel has a much greater selectivity than the Na channel (about 100:1 for K^+ over Na^+).

References

1. Kao CY. Structure-activity relations of tetrodotoxin, saxitoxin and analogues. Ann NY Acad Sc 1986; 479: 52-67.
2. Strichartz G, Rando T, Hall S, et al. On the mechanism by which saxitoxin binds to and blocks sodium channels. Ann NY Acad Sci 1986: 479: 96-112.
3. Narahashi T, Moore JW, Posten RN. Tetrodotoxin derivatives: chemical structure and blockage of nerve membrane conductance. Science 1967; 156: 976-9.
4. Hille B. The receptor for tetrodotoxin and saxitoxin. A structural hypothesis. Biophys J 1975; 15: 615-9.
5. Doyle DD, Guo YG, Lustig SL, Satin J, Rogart RB, Fozzard HA. Divalent cation competition with ^{3}H-saxitoxin binding to tetrodotoxin-resistant and -sensitive sodium channels. A two-site structural model of ion/toxin interaction. J Gen Physiol 1993; 101: 153-82.
6. Satin J, Limberis JT, Kyle JW, Rogart RB, Fozzard HA. The saxitoxin/tetrodotoxin binding site on the cloned rat brain IIa Na channel is in the transmembrane electric field. Biophys J 1994; 67: 1007-14.
7. Ritchie JM, Rogart RB. The binding of saxitoxin and tetrodotoxin to excitable tissue. Rev Physiol Biochem Pharmacol 1977; 79: 1-50.
8. Cohen CJ, Bean BP, Colatsky TJ, Tsien RW. Tetrodotoxin block of sodium channels in rabbit Purkinje fibers. J Gen Physiol 1981; 78: 383-411.
9. Salgado VL, Yeh JZ, Narahashi T. Use- and voltage-dependent block of the sodium channel by saxitoxin. Ann NY Acad Sci 1986; 279: 84-95.
10. Satin J, Kyle JW, Chen M, et al. A mutant of TTX-resistant cardiac sodium channels with TTX-sensitive properties. Science 1992; 256: 1202-5.
11. Guo Z, Uehara A, Ravindran A, Bryant SH, Hall S, Moczydlowski E. Kinetic basis for insensitivity to

tetrodotoxin and saxitoxin in sodium channels of canine heart and denervated rat skeletal muscle. Biochem 1987; 26: 7346–556.

12. Roy ML, Narahashi T. Differential properties of tetrodotoxin-sensitive and tetrodotoxin-resistant sodium channels in rat dorsal root ganglion neurons. J Neuroscience 1992; 12: 2104–11.
13. Noda M, Shimizu S, Tanabe T, et al. Primary structure of electrophorus electricus sodium channel deduced from cDNA sequence. Nature 1984; 312: 121–7.
14. Goldin AL. Voltage-gated sodium channels. In: North, RA, editor. CRC Handbook of Receptors and Channels, CRC Press; Boca Raton, FL, Vol. II. 1994, 73–112.
15. Satin J, Kyle JW, Chen M, Rogart RB, Fozzard HA. The cloned cardiac sodium channel α-subunit expressed in *Xenopus* oocytes show gating and blocking properties of native channels. J Membrane Biol 1992; 130: 11–22.
16. Catterall WA. Cellular and molecular biology of voltage-gated sodium channels. Physiol Rev 1992; 72: S15–48.
17. Guy HR, Seetharamulu P. Molecular model of the action potential sodium channel. Proc Nat'l Acad Sci USA 1986; 83: 508–12.
18. Terlau H, Heinemann SH, Stühmer W, et al. Mapping the site of block by tetrodotoxin and saxitoxin of sodium channel-II. FEBS Lett 1991; 293: 93–6.
19. Schild L, Moczydlowski E. Competitive binding interaction between Zn^{2+} and saxitoxin in cardiac Na^+ channels-Evidence for a sulfhydryl group in the Zn^{2+} saxitoxin binding site. Biophys J 1991; 59: 523–37.
20. Backs P, Yue D, Lawrence J, Marban E, Tomaselli G. Molecular localization of an ion-binding site within the pore of mammalian sodium channels. Science 1992; 257: 248–51.
21. Heinemann SH, Terlau H, Imoto K. Molecular basis for pharmacological differences between brain and cardiac sodium channels. Pflugers Arch 1992; 422: 90–2.
22. Lipkind GM, Fozzard HA. A structural model of the tetrodotoxin and saxitoxin binding site of the Na^+ channel. Biophys J 1994; 66: 1–13.
23. Hille B. The permeability of the sodium channel to organic cations in myelinated nerve. J Gen Physiol 1971; 58: 599–619.
24. Heinemann SH, Terlau H, Stühmer W, Imoto K, Numa S. Calcium channel characteristics conferred on the sodium channel by single mutations. Nature 1992; 356: 441–3.
25. Kirsch GE, Alam M, Hartmann HA. Differential effects of sulfhydryl reagents on saxitoxin and tetrodotoxin block of voltage-dependent Na channels. Biophys J 1994; 67: 2305–15.
26. Dudley SC, Todt H, Lipkind G, Fozzard HA. A μ-conotoxin-insensitive Na channel mutant: possible localization of a binding site at the outer vestibule. Biophys J 1995; 69: 1657–65.
27. Perez-Garcia MT, Chiamvimonvat N, Marban E, Tomaselli GF. Structure of the sodium channel pore revealed by serial cysteine mutagenesis. Proc Natl Acad Sci 1996; 93: 300–4.
28. Lipkind GM, Hanck DA, Fozzard HA. A structural motif for the voltage-gated potassium channel pore. Proc Natl Acad Sci USA 1995; 92: 9215–9.
29. Fozzard HA, Hanck DA. Structure and function of voltage-gated sodium channels: a comparison of Brian II and cardiac isoforms. Physiol Rev 1996; 70: 887–926.